Historical Shoreline Analysis

For Humboldt Bay, California

Shoreline Change along Coastal Dunes from Table Bluff to Trinidad, 1939-2016

Kelsey McDonald
October 10, 2017

Summary

The Historical Shoreline Analysis provides information on long-term trends in shoreline movement to support understanding of coastal change along dune systems within the Eureka littoral cell. The study is a component of the Dunes Climate Ready project, which seeks to understand how sea level rise will impact dune systems and how land managers can promote adaptation. Shorelines digitally traced from aerial imagery dating 1939 to 2016 revealed varying patterns of erosion and accretion across dune-backed shorelines of the Humboldt Bay area. The ArcGIS plugin Digital Shoreline Analysis System (DSAS) analyzed shoreline change along digital transects to provide linear regression rates of shoreline change over the study period. Most of the sandy shorelines around Humboldt Bay are stable to prograding, with the exception of the North Jetty area. The beach at the North Jetty has been eroding rapidly since 1939 (2.08 ± 0.16 m/year). The North Spit from Samoa to Mad River Beach has been stable to accreting (no significant change to less than 1m/year). The Clam Beach to Little River shoreline stretch has shown high accretion (2.56 ± 0.15 m/year). The South Spit has shown moderate accretion (1.27 ± 0.06 m/year). The long-term rates of change provide historical reference for monitoring coastal responses to sea level rise and climate events.

Introduction

The Historical Shoreline Analysis is a component of the Dunes Climate Ready Study, which seeks to provide information on patterns of sediment movement within the Eureka littoral cell and identify potential coastal vulnerabilities and responses to sea level rise and other aspects of climate change. Dunes of the Eureka littoral cell stretch 54km from Little River to Centerville Beach. The Historical Shoreline Analysis shows long-term shoreline change trends by tracing the shoreline along the foredune base (toe) from available aerial imagery taken over the past three-quarters of a century. This analysis covers the northern portion of the littoral cell surrounding Humboldt Bay from Little River State Beach to Table Bluff, and it will be supplemented by a similar analysis of the Eel River area.

Foredune Morphology and Processes

Foredunes are dynamic seaward dune ridges running parallel to the shore that can form along sandy shorelines above the typical reach of tides and wave swash (Hesp 1983, 2002, 2013). Foredunes are created by aeolian sand deposition in vegetation or other roughness elements (Hesp 1983, 2002, 2013). Vegetation growth is limited at the seaward edge by high spring tide and storm swash, and this zone marks the transition from upper beach to foredune (Hesp 2013). The transition zone where the slope increases from the upper beach is the foredune toe. Storm-induced wave heights, especially coinciding with spring tides, can erode sand from the toe of the foredune, causing scarping (cliffing) and moving the foredune toe inland (Battiau-Queney 2003, Hesp 2013, Pickart 2014). Erosion from the base of the foredune is typically followed by the formation of aerodynamic sand ramps that, in the absence of vegetation, allow sand deposition over the crest of the dune, one mechanism by which foredunes translate inland as sea levels rise (Davidson-Arnott 2005, Hesp 2002, Hesp 2013).

The Humboldt Bay area contains many sediment-supplying rivers and streams. Major sources of sediment include the Little River, the Mad River, and the Eel River, which discharge 53,000, 486,000, and 2,300,000 m^3/year of sediment, respectively (Patsch and Griggs 2007). Although the Eel River discharges more than twice as much sediment as any other river in California, an unknown quantity is lost to submarine canyons offshore, making the sediment budget for the Eureka littoral cell difficult to estimate (Hapke et al. 2006, Patsch and Griggs 2007). The direction of littoral drift may vary by season, year, and location within the Eureka littoral cell (Patsch and Griggs 2007, Moffat & Nichol 2013). Sediment availability and deposition patterns are complicated by human engineering as well, including the jetties at the entrance to Humboldt Bay and management of dredged materials from the bay.

Sea Level

Comparing long-term global sea level rise with shorter-term changes shows that the rate of sea level rise has increased. Global mean sea level has risen more quickly since the mid-19th century than has been seen over the previous two millennia (IPCC 2014). The current rate of global sea level rise is very likely to increase over the 21st century (IPCC 2014). Rates of sea level rise differ by location because of variation in the earth's gravitational field, changing ocean currents, and tectonic movement (IPCC 2014). Humboldt Bay's North Spit tide gauge shows a higher relative sea level rise rate than any other gauge on the Pacific Coast of North America (Appendix B: Figure 1) (NOAA CO-OPS, Accessed July 2017). Tide gauge analysis and land-level surveys have shown subsidence along the coast of the Humboldt Bay area (Patton et al. 2017). Humboldt Bay is located in the tectonically active southern end of the Cascadia Subduction Zone near the junction of the Pacific Plate, North American Plate, and Gorda Plate at Cape Mendocino, and vertical land motion compounds the rate of sea level rise in the Humboldt Bay area (Patton et al. 2017).

Sea level is subject to seasonal, interannual, and interdecadal variation. Sea levels vary in a predictable way over the course of the year, with highest ocean temperatures and sea levels occurring during the winter in the Pacific Northwest (Appendix B: Figure 2) (NOAA CO-OPS, Northern Hydrology 2015). Spring upwelling brings cooler, more fertile water to the Pacific coast, causing a seasonal drop in sea level. El Niño Southern Oscillation (ENSO) events, which are characterized by warmer ocean temperatures, increase sea level along the Pacific coast (NRC 2013). Average wave heights are greatest during the winter on the North Coast (Hapke 2006). During El Niño winter months, wave heights are elevated 0.3-1.2m (Hapke 2006). La Niña can also elevate wave heights to the North Coast by 0.1m-0.4m (Hapke 2006). The Pacific Decadal Oscillation (PDO) is a longer-term cycle between warm and cool phases in ocean temperatures that also affects sea-level. Local sea level also varies on a daily basis with tides, wave height, and storm surge. The many cycles affecting sea level can compound to produce exceptionally high seas when cycles are in the same phase (Cayan et al. 2008). Increases in sea level magnify the impact of storm surge and high waves on the coast (NRC 2013). Climate-related events can cause short term variability in shoreline position, or they can have a lasting impact (e.g., Barnard et al. 2009).

Measuring Shoreline Change

The United States Geological Survey (USGS) has conducted several studies of shoreline change in coastal areas across the United States as part of the National Assessment of Shoreline Change (Morton et al. 2004, Morton et al. 2005, Hapke et al. 2006, Hapke and Reid 2007, Hapke et al. 2010, Fletcher et al. 2012, Gibbs and Richmond 2015). The USGS has used Digital Shoreline Analysis System (DSAS), a software extension for ESRI ArcGIS, to calculate rates of shoreline change. In the 2006 study of shoreline change along sandy shorelines of California, USGS used Mean High Water (MHW) derived from historical maps and LiDAR as an indicator for shoreline (Hapke et al. 2006). The USGS study found an overall long term accretion trend of 0.2 +/-0.1 m/year (dating to the 1800s) and a short term erosion trend of -0.2 +/-0.4 m/year (1950s-70s to 1998-2002) along the sandy shorelines of California. The USGS study found a 0.7m/year long term accretion trend along sandy shores of the Eureka littoral cell (1854-70 to 2002), although a large data gap occurred along the bulk of the north and south spits of Humboldt Bay. Long term erosion areas occurred along only 4% of the measured coast in the

Eureka littoral cell, and averaged -0.2m/year. The highest erosion in the area was recorded on the North Spit of Humboldt Bay 0.8km north of the jetty as -2.7m/year from 1956-68 to 2002 (Hapke et al. 2006).

Both the U.S. Army Corps of Engineers (USACE) and U.S. Fish and Wildlife (USFWS) have studied shoreline movement in the Humboldt Bay area. The USACE analyzed shoreline change over a study area that extended 7 miles on either side of the jetties from 1992-2015 (USACE 2012, USACE 2017). The study used flyover imagery and LiDAR on the North and South Spits to monitor movement of an upper beach reference line as part of the Humboldt Shoreline Monitoring Program (USACE 2012). The USACE study found that the shoreline around the North Jetty was rapidly eroding in the 1990s, followed by a period of accretion that brought the 2015 shoreline nearly back to the 1992 starting point (USACE 2017). The beach around the South Jetty showed overall accretion (USACE 2012, USACE 2017). The USACE concluded that the latest 2011-2015 study period was a period of widespread beach growth on North and South Spits (USACE 2017). A similar pattern was observed in the USFWS study, which found that 1998-2000 was a period of widespread erosion along the North Spit study area, which extended from Manila to Lanphere Dunes (Pickart 2014). The USFWS study found lesser erosion over the 2000-2012 study period (Pickart 2014). The agency studies are limited in time to the last few decades and do not cover the entire coast of the Humboldt Bay area.

The Historical Shoreline Analysis fills spatial and temporal gaps in the previous studies of shoreline change along the Eureka littoral cell. The USGS study of change along sandy shorelines of California provided a broad analysis of shoreline change patterns across the state; however the data sources used in the study were not available for a significant portion of the Eureka littoral cell, with a gap in data along the spits of Humboldt Bay (Hapke et al. 2006). The USGS study was also limited by time interval, with three shorelines digitized from available t-sheets representing each of the 1800s, 1920s-30s, and 1950s-70s, and a current shoreline extracted from post-1998 LiDAR (Hapke et al. 2006). The Historical Shoreline Analysis for the Dune Climate Ready Study aims to provide more complete coverage of sandy shorelines of the Humboldt Bay area and to provide more detailed information on patterns of shoreline change than the broader statewide study could provide. Like the USGS National Assessment of Shoreline Change, the Historical Shoreline Analysis uses DSAS to calculate rates of shoreline change along transects, but data sources and shoreline indicators differ from the USGS study.

Defining the Shoreline

Studies of shoreline change have used a wide range of indicators to delineate the shoreline. The USGS National Assessment of Shoreline Change used the Mean High Water (MHW) line, and the Army Corps of Engineers used an upper beach reference line. Boak and Turner (2005) found 19 different generic shoreline indicators in a review of 45 shoreline change studies, highlighting the importance of thoroughly defining the shoreline and delineation methods. Common shoreline indicators along sandy shores have included the high-water line, scarp line, the seaward dune vegetation line, mean high water, instantaneous water line, and the debris line (Boak and Turner 2005). The high water line is a widespread indicator, but it has many potential problems. Wave run-up and tides can cause the high water line to vary by many meters on a daily basis (Pajak and Leatherman 2002). Storms can cause the high water line to migrate up to 100m (Leatherman cited in Moore 2000). Because of the high variability of the high water line, it may be better to use more stable features such as the bluff/dune toe or vegetation line in areas where these features exist (Morton 1991; Thieler and Danforth 1994)**.** Dune toe is a common shoreline proxy in areas where dune features are present because it is less dependent on meteorological conditions (Del Río and Gracia 2013), e.g., (Barnard et al. 2009; Battiau-Queney et al. 2003; Chaaban et al. 2012).

Battiau-Queney (2003) used a similar method of measuring shoreline change using the foredune toe as a shoreline proxy along sandy beaches in the north of France. The dune morphology along the study area in the north of France was similar to sandy shores of the Eureka littoral cell, with 10-20m-high foredunes dominated by European beach grass (*Ammophila arenaria*). In the field, Battiau-Queney (2003) defined the foredune toe as the "more or less sharp break of slope from the gentle upper beach to the steep dune front." Embryo dunes associated with sea rocket (*Cakile maritima*) were considered to be part of the beach. The study determined the foredune toe stereoscopically from orthorectified aerial imagery (Battiau-Queney et al. 2003). In a later shoreline change study in the north of France, Chaaban et al. (2012) delineated the toe of the foredune from georeferenced aerial photographs (Chaaban et al. 2012).

Shoreline Variability and Error

Although foredunes to not fluctuate as dramatically as the high water line, the toe of the foredune is dependent on sea-level and can vary seasonally or interannually (Hesp 2013). Foredunes reflect short-term, medium-term, and long-term processes occurring in the beach-dune system (Hesp 2002). In Humboldt Bay, the foot of the foredune typically coincides with the vegetation line, where European beachgrass, American dunegrass, and other foredune plants grow fairly continuously. Foredune foot is not a true linear feature, but a zone of transition from upper beach where the slope begins to steepen and build into a foredune (as observed by Battiau-Queney et al. 2003, see Appendix A). The foot of the foredune can be visualized as the location one could mark the seaward edge of foredune while walking along the beach. Along the coast of Humboldt Bay, the foot of the foredune was observed to typically coincide with 6m elevation NAVD88 (McDonald 2014), which is approximately 4m above MHHW (NOAA vDatum, accessed July 2017). The upper 20% of winter wave heights in Northern California reach 4m or higher (Hapke et al. 2006), potentially bringing these larger waves just in reach of the foredune toe at higher high tide.

Temporary and seasonal variations (with more scarping occurring during winter storms, and ramping occurring during the summer) can be a source of error in determining long-term trends. The influence of outliers in shoreline position caused by short-term variability in determining long-term trends can be reduced by limiting the imagery used to a particular season and excluding post-storm imagery (Moore 2000). Seasonal and post-storm variation is reduced by using the foredune toe compared to the high-water line, but it is still a potential source of error. Most of the aerial imagery used in this study was flown during the summer and early fall, with the exceptions of the imagery used for the earliest shoreline (1939 in the southern two-thirds of the study area and 1941/42 from the Mad River Beach to Little River) and imagery from 1999 (Appendix B: Figure 1). Winter imagery was included to fill in a temporal gap in the data in the 1990s and to include the earliest available imagery. The relatively large shoreline sample size (n=10 years) of shorelines used in linear regression rate for this study reduces the influence of short-term anomalies in shoreline position, which are assumed to be random and normally distributed. Results calculated for individual intervals using *end point rate* are more vulnerable to non-independent operator and georeferencing errors, and should be interpreted with more caution.

Objective

The objective of the historical shoreline analysis study is to show patterns of erosion or accretion that have occurred along the sandy shorelines of the northern portion of the Eureka littoral cell over the last 77 years. This study utilizes the toe of the foredune traced from aerial imagery as a proxy to measure long-term shoreline change. The study also provides baseline conditions for monitoring future movement of the shoreline, and a history of shoreline movement for interpreting ongoing studies of dune translation in the area.

Methods

Aerial Imagery

The Historical Shoreline Analysis used aerial imagery for the Humboldt Bay area coast that was available from 1939-2016 at approximately decadal time intervals. The study area covered the dunes of the Humboldt Bay area from Table Bluff north to Little River State Beach (Figure 1). Imagery was acquired for the years 1939/1941/42, 1948, 1958, 1965, 1970, 1981, 1988, 1999, 2005, and 2016. Imagery sources included historical aerial imagery obtained from Humboldt County Public Works Department that was scanned and georeferenced, previously orthorectified aerial mosaics from the Humboldt Bay - Eel River Historic Atlas, and modern digital orthoimagery from the National Agricultural Imagery Program (NAIP) and National Digital Ortho Photo Program (NDOP) (Appendix B: Table 1). The Humboldt Bay – Eel River Historic Atlas extends from the Eel River Estuary to the Mad River, and it does not include the dune systems from Mad River north to Little River Beach (Laird 2007). Historical aerial imagery of the northern portion of the study area was georeferenced using ESRI ArcMap for the years 1948-1981 to supplement imagery from the Humboldt Bay – Eel River Historic Atlas. Georeferencing methods followed those outlined by Thieler and Danforth (1994), using pass points between images where ground control points from the reference imagery (2012 NAIP) were unavailable. At least 30 total ground control and pass points were used to georeferenced the aerial photographs, and a spline transformation was applied. Imagery for 1988 was available as a mosaic from the National Digital Ortho Photo Program (NDOP). The imagery for 1939, 1941/42, and 1999 was georeferenced for their entire extents along the Humboldt Bay area sandy coastlines. The imagery for 1939 does not include the area north of Lanphere Dunes, and the imagery for 1941/42 does not include the southern portion of the South Spit. The earliest available imagery was used as the start date for statistical analysis; imagery from 1939 was used for the South and North Spits, and imagery from 1941/42 was used for the northern portion of the study area. Imagery for the two most recent years, 2005 and 2016, came from the National Agriculture Imagery Program (NAIP).

Shoreline Delineation

This study followed a similar method to those used by Battiau-Queney (2003) and Chaaban et al. (2012) of delineating the foredune toe from georeferenced and orthorectified aerial photography, including the bases of continuously vegetated incipient dunes and foredune scarps. Small, isolated incipient dunes or nebkha near the ocean formed by sea rocket (*Cakile spp.*) and other species that do not form a mostly continuous perennial linear shoreline feature were not included. The toe of the foredune was identified in aerial photographs by looking for the foredune vegetation line or topographical relief at the edge of the foredune.

The foredune toe was digitally traced three times on all imagery mosaics using ESRI ArcMap software for all years and the three lines were averaged to reduce error. Vertices were placed as needed to delineate the toe of the foredune, approximately every 50-100m while inspecting the imagery at a 1:3000 scale. The shoreline as drawn is intended to reflect long-term changes in accretion or erosion, so small scale temporary features (up to 200m) like blowouts were interpolated (i.e. a continuous line drawn along the mouth of the blowout lined up with the foredune toe to the north and south). In areas that were challenging to interpret, the shoreline delineation was checked and edited using a stereoscope with aerial photographs to look for relief displacement. Shorelines were segmented to exclude any larger areas that could not be interpreted, including river mouths, overwash areas, and other breaks in the foredune. Ground-truthing the 2016 shoreline by walking the toe of the foredune with a GPS unit showed that the methods of remotely delineating the foredune toe from aerial imagery were accurate to within an average distance of ~3m at all checked locations (See Appendix C: Ground Truth Report 2016, Table 1).

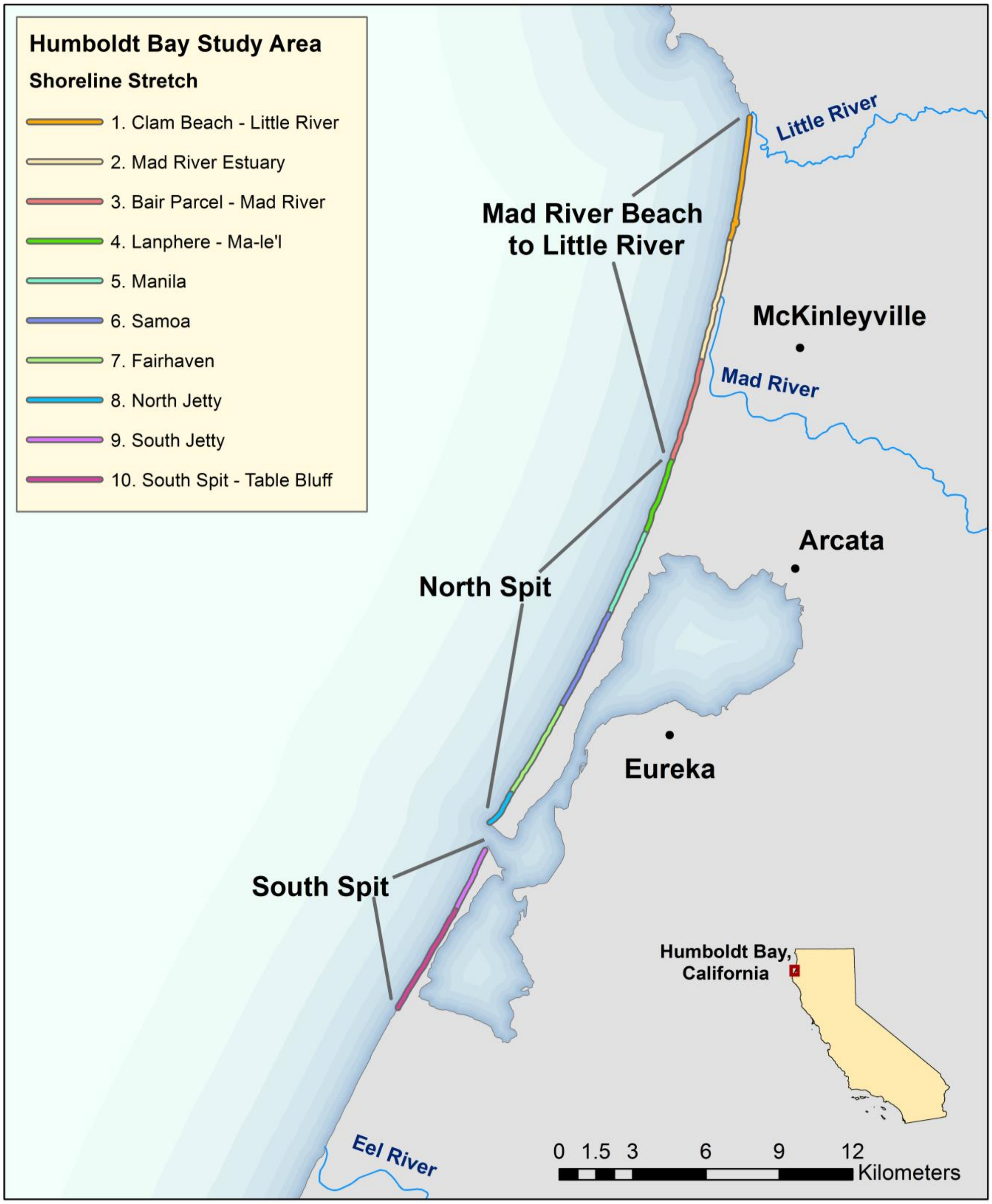

Figure 1. The Humboldt Bay study area was divided into three broad locations: Mad River Beach to Little River, North Spit, and South Spit. Each of the broad locations was divided into smaller shoreline stretches to provide more specific information on patterns of shoreline change.

Analysis

Digital Shoreline Analysis System (DSAS) v. 4.3, a software extension for ESRI ArcGIS, was used to calculate rates of shoreline change using the single transect method (Thieler et al. 2017). A 500m buffer of all years' shorelines was edited to obtain a generalized baseline offshore from the shorelines. Transects were cast perpendicular to the baseline at 100m intervals with a 500m smoothing factor using DSAS software. Three shorelines were traced for each year, and average shorelines for each year were calculated from the intersections of the three traced shorelines with each transect. Calculating the average of the three traced shorelines provided an improved assessment of the position of the foredune foot, and it provided a way to quantify the human error in interpreting and digitizing shorelines (i.e digitizer error (E_d)) from aerial imagery.

Digital Shoreline Analysis System (DSAS) calculated the shoreline change statistics *linear regression rate* and *net shoreline movement* for each transect over the study period 1939-2016 (where 1939 imagery was available) or 1941/42-2016 (Table 1). Linear regression is a common method of calculating shoreline change where sufficient data from multiple time periods are available, and it is used by the National Assessment of Shoreline Change for calculating long-term rates of change (Hapke et al. 2006). The slope of the line fit through the positions of the shoreline over time provides the rate of shoreline change (Himmelstoss 2009). The intersection threshold was set equal to the total number of years to be used in the analysis so that areas with gaps in the shoreline digitized for any year would not be used in the analysis. The shoreline change statistic *end point rate* was then calculated using DSAS for each interval between years (Table 2). Statistics calculated for each transect using DSAS were then averaged by shoreline stretch and over the entire study area to provide average rates of change for specific shoreline stretches as well as overall rates of change for the study area.

Uncertainty calculations were derived from USGS National Assessment of Shoreline Change methods developed by Hapke and others (2006). The error in shoreline position (E_{sp}) was calculated using the root sum of square errors that derive from measurement errors and physical uncertainty in delineating shorelines: georeferencing error (E_g), digitizing error (E_d), and shoreline position error (E_p) (Equation 1). Georeferencing error (E_g) was estimated to be 10m. All scanned aerial photos were georeferenced in ArcMap 10.3 with a first order polynomial transformation RMSE on the order of 10m prior to selecting a spline transformation, which causes the RMSE calculation to go to zero. Digitizing error (E_d), was calculated using the 95% confidence interval, calculated using twice the standard deviation, from tracing each shoreline three times. Shoreline position error (E_p) was estimated to be 3m, based on the observed uncertainty of identifying the true physical location of the foredune toe feature while walking the beach (See Appendix C: Ground Truth Report 2016).

Equation (1)

$$E_{sp} = \sqrt{E_g^2 + E_d^2 + E_p^2}$$

The shoreline position uncertainty values were used to calculate end point rate confidence intervals (*ECI*) in DSAS according to Equation 2 (Himmelstoss 2009). The error in the long-term linear regression rates of shoreline change along individual transects is the 95% confidence interval. The reported uncertainties for all averaged transect rates (U_{Avg}) were calculated using root mean square error, as described in Gibbs and Richmond (2015) (Equation 3). Multiplying the averaged end point rate confidence intervals by the time interval provided the uncertainty in net shoreline movement.

Equation (2)

$$ECI = \frac{\sqrt{E_{sp1} + E_{sp2}}}{year_2 - year_1}$$

Equation (3)

$$U_{Avg} = \frac{\sqrt{\sum_{i=0}^{n} E_i}}{n}$$

Results

The dune-backed sandy shores of the Humboldt Bay area have shown an average pattern of minor accretion (0.51 ± 0.03 m/year) over the past eight decades (Table 1). Most of the shoreline has been prograding toward the sea, with 70% of all transects showing accretion, followed by 22% showing no significant change, and only 7% showing erosion. However, inspecting the shoreline change over smaller stretches of the shoreline shows variable localized patterns (Figures 2-3). The highest accretion occurred in the northern portion of Little River Beach, where the maximum accretion was 4.24 m/year (Appendix A: Figure 1). Of the three major subareas, the northernmost stretch of shoreline from Clam Beach to Little River Beach showed the highest average accretion, with 2.56 ± 0.15 m/year (Appendix A: Figure 2). Rate of change was not uniform over the North Spit. The shoreline from Mad River Beach to Samoa along the North Spit of Humboldt Bay was stable to accreting (Appendix A: Figures 3-5). Near Fairhaven, shoreline change switched to an erosive pattern (Appendix A: Figure 6). The North Jetty shoreline showed the highest erosion, with an average rate of -2.08 ± 0.16 m/year (Appendix A: Figure 7). The pattern of shoreline change switched back to accretion at the South Jetty, and the southern subarea (South Spit) showed medium accretion (1.27 ± 0.06 m/year) from the jetty to Table Bluff (Appendix A: Figures 8-9).

Rates of shoreline change and percentage of transects eroding/accreting also varied by time interval (Table 2). The first time interval 1939-1941/42 showed high average erosion (-2.66 m/year), with 69% of transects eroding over the study area where imagery was available (from the South Spit to Lanphere Dunes). Erosion at the North Jetty was extreme during this time period—nearly -20 m/year. The following interval 1941/42-1948 showed high average accretion (2.65 m/year) over the entire study area. Subsequent time intervals showed no significant change to medium accretion over the entire study area until 1970 (Table 2). Both 1970-1981 and 1988-1999 were periods of overall erosion (Table 2). The North Spit showed a period of erosion from 1981-2005. The North Spit switched to a significant period of accretion during the most recent time period 2005-2016, with the exception of the erosive North Jetty and Fairhaven areas. The South Spit was stable to accreting over the entire study period with the exception of the erosive 1970-1981 time period (Table 2).

Table 1. The net shoreline movement (m) and linear regression rates (m/year) of shoreline change show overall patterns of accretion and erosion for each location between 1939 and 2016. Imagery for 1939 was not available for the Mad River Beach to Little River study area, and overall rates for this location are for 1941/42-2016. Blue text indicates that the linear regression rate shows accretion, and red indicates erosion. The percent of transects showing significant erosion, significant accretion, and no significant change at the 95% confidence level are provided. Error values provided in the table (±) reflect uncertainty of the averaged rates (U_{Avg}) (see Equation 3). Locations in the table are depicted in Figure 1.

Location	Latitudes	n	Net Shoreline Movement (m)		Linear Regression Rate (m/yr)		% Erosion	% Accretion	% No Change
Overall Humboldt Bay Study Area	40°41'49"N - 41°1'35"N	271	48	± 1	0.51	± 0.03	7%	70%	22%
Mad River Beach to Little River	**40°53'57"N - 41°1'35"N**	**54**	**97**	**± 2**	**1.19**	**± 0.07**	**0%**	**85%**	**15%**
Clam Beach to Little River	40°58'50"N - 41°1'35"N	21	197	± 4	2.56	± 0.15	0%	100%	0%
Bair Parcel to Mad River Beach	40°53'57"N - 40°56'9"N	33	33	± 3	0.31	± 0.05	0%	76%	24%
North Spit to Mad River Beach	**40°45'53"N - 40°53'56"N**	**159**	**11**	**± 1**	**0.01**	**± 0.04**	**13%**	**55%**	**33%**
Lanphere to Ma-le'l	40°52'21"N -40°53'56"N	31	28	± 3	0.32	± 0.03	0%	100%	0%
Manila	40°50'34"N - 40°52'20"N	36	46	± 3	0.55	± 0.03	0%	94%	6%
Samoa	40°48'29"N - 40°50'33"N	41	38	± 2	0.40	± 0.07	0%	54%	46%
Fairhaven	40°46'33"N - 40°48'28"N	39	-8	± 4	-0.51	± 0.13	21%	0%	79%
North Jetty	40°45'53"N - 40°46'33"N	12	-174	± 5	-2.08	± 0.16	100%	0%	0%
South Spit	**40°41'49"N - 40°45'18"N**	**58**	**106**	**± 2**	**1.27**	**± 0.06**	**0%**	**100%**	**0%**
South Jetty	40°43'59"N - 40°45'18"N	22	126	± 4	1.47	± 0.09	0%	100%	0%
South Spit to Table Bluff	40°41'49"N - 40°43'58"N	36	93	± 3	1.14	± 0.08	0%	100%	0%

Table 2. End point accretion or erosion rates (m/year) show shoreline change over each time interval for each location. Blue text indicates accretion, and red indicates erosion. Error values (±) reflect the uncertainty of the averaged end point rates (U_{Avg}) (see Equation 3), which was calculated using end point rate confidence interval (ECI) (see Equations 1-2).

End Point Rate Accretion (+) or Erosion (-) of Shorelines by Interval (m/year)

Location	1939-1941/42	1941/42-1948	1948-1958	1958-1965	1965-1970	1970-1981	1981-1988	1988-1999	1999-2005	2005-2016
Overall Humboldt Bay Study Area	-2.66 ± 0.04	2.65 ± 0.16	0.67 ± 0.11	0.89 ± 0.15	1.64 ± 0.23	-0.15 ± 0.09	1.42 ± 0.14	0.02 ± 0.08	-0.01 ± 0.15	1.29 ± 0.08
Mad River Beach to Little River	—	**2.84 ± 0.28**	**0.66 ± 0.18**	**0.80 ± 0.27**	**2.91 ± 0.41**	**0.10 ± 0.18**	**3.69 ± 0.28**	**0.65 ± 0.15**	**0.27 ± 0.29**	**1.74 ± 0.15**
Clam Beach to Little River	—	5.31 ± 0.48	0.49 ± 0.33	3.61 ± 0.40	4.28 ± 0.70	-0.17 ± 0.33	8.46 ± 0.45	1.99 ± 0.23	0.90 ± 0.45	4.00 ± 0.26
Mad River Beach	—	2.54 ± 0.47	1.06 ± 0.31	-0.45 ± 0.52	1.96 ± 0.72	-0.08 ± 0.24	0.17 ± 0.39	-0.49 ± 0.22	-0.57 ± 0.41	0.46 ± 0.21
North Spit to Mad River Beach	**-3.83 ± 0.05**	**2.82 ± 0.23**	**0.94 ± 0.15**	**0.50 ± 0.22**	**0.95 ± 0.31**	**0.06 ± 0.12**	**-1.29 ± 0.19**	**-0.78 ± 0.11**	**-0.82 ± 0.21**	**0.35 ± 0.11**
Lanphere to Ma-le'l	-2.20 ± 0.08	1.06 ± 0.52	0.83 ± 0.35	-0.18 ± 0.48	0.47 ± 0.70	0.79 ± 0.30	0.11 ± 0.46	-0.16 ± 0.25	-0.60 ± 0.49	1.17 ± 0.26
Manila	0.37 ± 0.09	0.27 ±0.45	0.72 ± 0.30	1.54 ± 0.41	0.65 ± 0.58	0.39 ± 0.25	0.90 ± 0.43	-0.31 ± 0.24	-0.12 ± 0.46	1.47 ± 0.24
Samoa	-1.49 ± 0.08	2.68 ± 0.40	1.84 ± 0.28	1.40 ± 0.45	0.79 ± 0.67	-0.32 ± 0.25	0.01 ± 0.36	-0.21 ± 0.20	-0.47 ± 0.41	0.04 ± 0.22
Fairhaven	-6.17 ± 0.12	8.04 ± 0.48	1.09 ± 0.31	-0.02 ±0.43	2.43 ± 0.58	-0.68 ± 0.23	-4.02 ± 0.37	-1.80 ± 0.21	-1.69 ± 0.42	-0.35 ± 0.22
North Jetty	-19.61 ± 0.21	-1.46 ± 1.04	-1.68 ± 0.59	-1.97 ± 0.82	-1.27 ± 1.12	1.03 ± 0.45	-6.95 ± 0.70	-2.32 ± 0.38	-1.78 ± 0.79	-1.64 ± 0.41
South Spit	**0.99 ± 0.07**	**1.74 ± 0.43**	**0.02 ± 0.26**	**1.9 ± 0.37**	**1.22 ± 0.57**	**-0.94 ± 0.21**	**4.87 ± 0.29**	**1.05 ± 0.16**	**1.43 ± 0.33**	**2.76 ± 0.18**
South Jetty	1.32 ± 0.10	3.59 ± 0.62	0.28 ± 0.45	0.51 ± 0.66	2.16 ± 0.98	-0.88 ± 0.34	3.31 ± 0.45	2.71 ± 0.27	1.64 ± 0.56	2.62 ± 0.30
South Spit to Table Bluff	0.67 ± 0.10	0.28 ± 0.59	-0.12 ±0.32	2.72 ± 0.45	0.67 ± 0.69	-0.98 ± 0.27	5.83 ± 0.37	0.03 ± 0.21	1.31 ± 0.40	2.85 ± 0.22
Percent Transects Eroding	69%	22%	22%	29%	33%	53%	32%	61%	48%	24%
Percent Transects Accreting	31%	78%	78%	71%	77%	47%	68%	39%	52%	76%

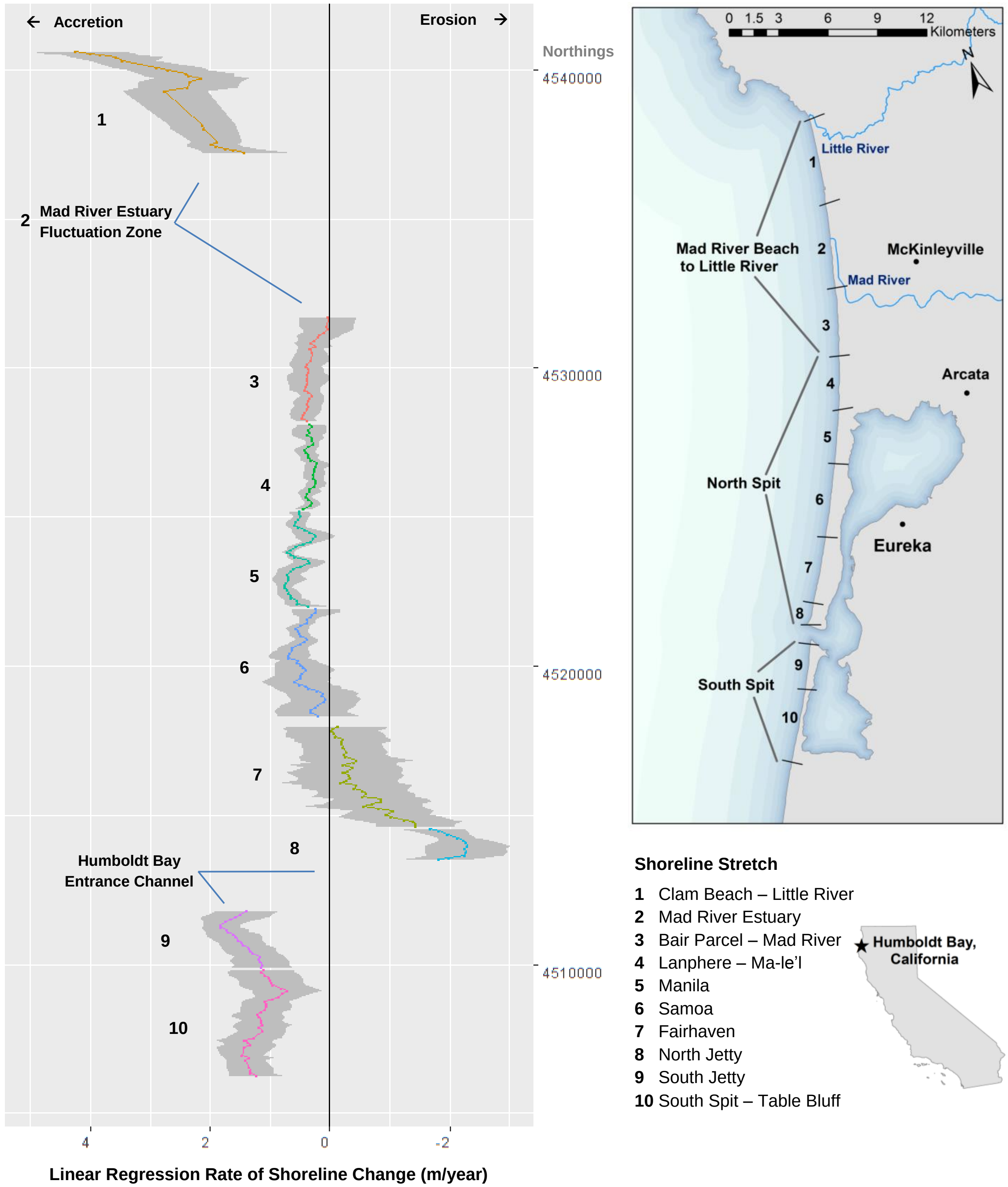

Figure 2. Linear regression rates of change along transects are plotted from north to south with the 95% confidence intervals shaded in grey. Areas where the 95% confidence intervals encompass zero are considered to show no significant change. Numbered shoreline stretches in the plot correspond to the map on the right. The northern portion of the study area from Clam Beach to Little River showed the highest rate of accretion. Most of the North Spit from Samoa up to Mad River Beach was stable to accreting, with the pattern switching to high erosion at the North Jetty. The South Spit (the South Jetty to Table Bluff) showed steady accretion.

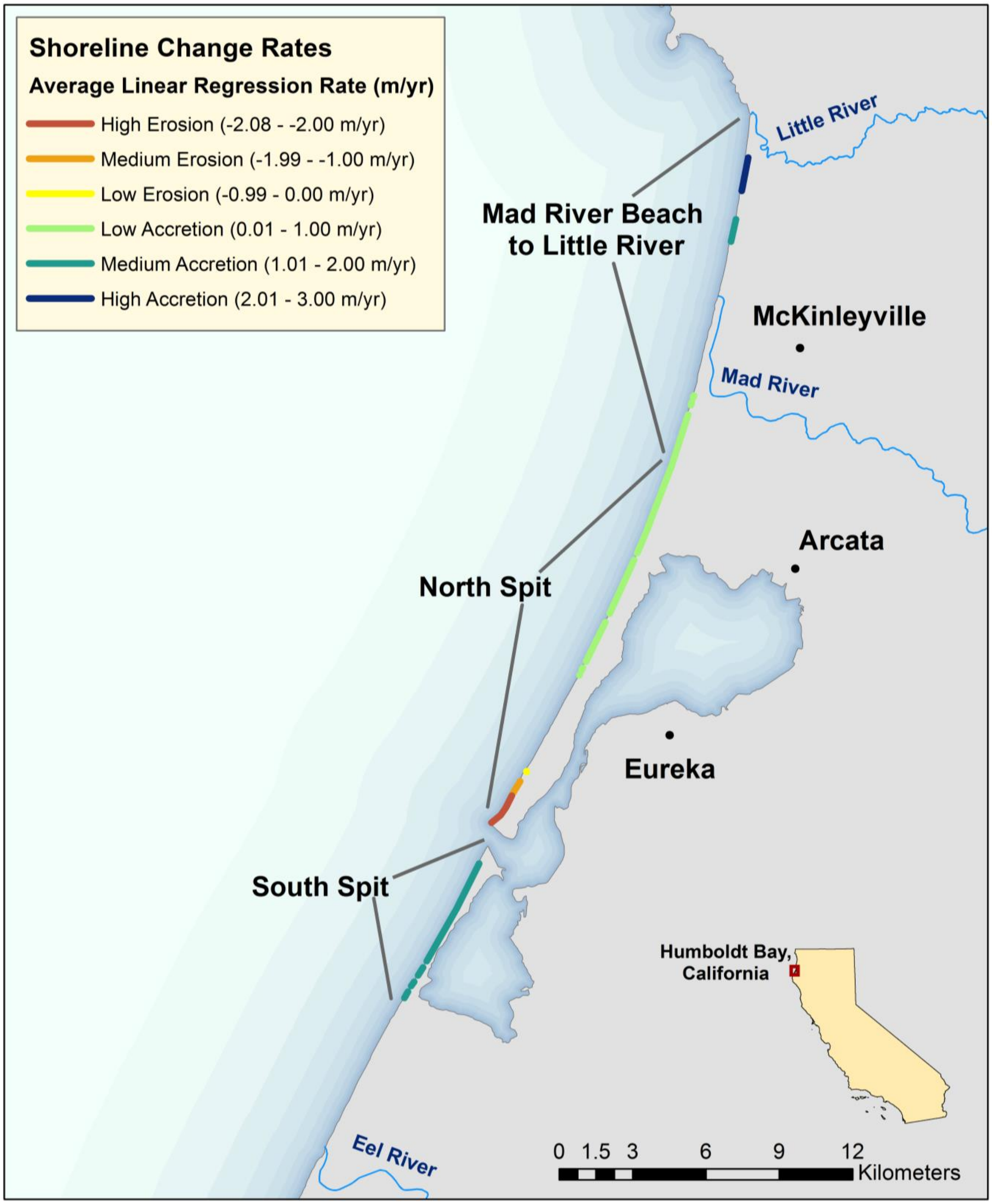

Figure 3. Average linear regression rates show general patterns of shoreline change rates over the Humboldt Bay study area. The northern-most study area Clam Beach to Little River showed medium to high average accretion. Study areas between Mad River Beach and Samoa showed no change to low accretion. Areas of insignificant change are not depicted, notably in the Fairhaven area, where the pattern transitioned from accretion to erosion. The North Spit between Fairhaven and the North Jetty showed increasingly high erosion toward the North Jetty. The South Spit of Humboldt Bay showed medium accretion.

Discussion

Over the nearly eight decades of the study period (1939-2016), most of the sandy shorelines of the Humboldt Bay area have been stable to accreting. The beach at North Jetty, which has eroded at an average rate of -2.08m/year, is a dramatic exception to the general trend of accretion. At the northern end of the study area, the Little River – Clam Beach area has experienced equally dramatic accretion at an average rate of 2.56m/year. The South Spit, which has shown accretion of 1.26m/year, has visibly widened since 1939 photos, which show a thin spit of land with areas where the waves wash over the spit into the bay.

Comparison with Previous Studies

The results of this study coincide with the overall changes documented by the USGS National Assessment of Shoreline Change and the Army Corps of Engineers erosion monitoring, when taking into the account the different time periods encompassed by these studies. Although the USGS National Assessment of Shoreline Change covered a much larger area, data was lacking altogether for most of the North and South Spits, and the areas covered used shorelines from only two dates for short-term rates and four dates for long-term rates (Hapke et al. 2006). The USGS study also found overall low accretion rates for the Eureka region, which they defined as the 74km stretch from Little River State Beach to Cape Mendocino. The USGS study found accretion of 0.7m/year between the late 1800s and 2002 and 0.4 m/year between 1956-68 and 2002 (Hapke et al. 2006), compared to 0.51 m/year between 1939-42 and 2016 found in this study. Both this study and the USGS study found the highest accretion at Little River State Beach, where the maximum rate was over 4m/year (Hapke et al. 2006). The USGS study found long term accretion at the North Jetty, but their data included maps from the late 1800s drawn prior to the building of the jetties and stabilization of the entrance to Humboldt Bay (Hapke et al. 2006). The USGS maximum short-term erosion rate of -2.7m/year (1956-68 to 2002) at the North Jetty was similar to the maximum rate of -2.29m/year (1939 to 2016) at the North Jetty found in this study.

The Army Corps of Engineers monitored for erosion along the North and South Spits from 1992-2015 (USACE 2017). The Corps documented extensive erosion along the North Spit during the 1992-2005, which was especially concentrated at the North Jetty (USACE 2012). By 2015, the North Spit had regained much of the area that was lost during the erosive period in the 1990s (USACE 2017). Likewise, the Historical Shoreline Analysis showed a period of erosion on the North Spit from 1981-2005, followed by accretion from 2005-2016. The Corps also documented overall accretion on the South Spit (USACE 2012), backing up the finding in this study that the South Spit has steadily accreted sediment since 1939. The USFWS finding of widespread erosion from Manila to Lanphere Dunes from 1998-2000 (Pickart 2014) also backs up erosional end point rate calculated along the North Spit 1999-2005, while the USFWS study interval 2000-2012 does not clearly correspond to a study interval in the Historical Shoreline Analysis.

Potential Mechanisms of Shoreline Movement

Potential drivers of the variable trends in shoreline movement include nearby sediment sources, littoral drift, tectonics, climate events, and human activities such as jetty construction and dredging. Jetty construction in the late-1800s dramatically changed sediment deposition around the entrance to Humboldt Bay. The difference can be seen in maps from that era available in the Humboldt Bay Atlas (Laird 2007). The jetties most likely still influence the patterns of littoral drift and sediment deposition in this area. Dredging from Humboldt Bay and deposition offshore decreases the availability of sediment within the littoral zone, and might decrease the potential for dunes and beaches to accrete sediment (Moffat & Nichol 2013). Previous nearshore disposal sites in use before 1990 may have influenced sediment deposition patterns as well (Moffat & Nichol 2013). Land-level surveys and tide gauge analysis have shown the coastal Humboldt Bay area subsiding, leading to local relative sea-level rise of two to three times the rate of anywhere in California (Patton et al. 2017). Rates of subsidence were highest in the southern part of Humboldt Bay (Patton et al. 2017), and a gradient in vertical land motion might influence patterns of shoreline change. High relative sea level rise in the Humboldt Bay area could pose an increased threat of shoreline erosion.

Rivers and streams supply more sediment to the Eureka littoral cell than any other littoral cell in California, although much of this may be lost to offshore submarine canyons (Hapke et al. 2006, Patsch and Griggs 2007). The Mad River has fluctuated over 4.75 km in the study period, alternately building and breaching a substantial sand spit at the mouth of the estuary (Appendix A: Figure 10). Sediment from the Mad River and Little River might play a role in the accretional shoreline trends seen in the northern part of the Humboldt Bay study area, especially in the Clam Beach to Little River Beach shoreline stretch, which has shown high accretion over the study period. The Eel River to the south of Humboldt Bay is a major source of sediment for the Eureka littoral cell, and might influence the accretional trend seen at the South Spit. Variable seasonal trends in littoral drift direction and sediment deposition within the Eureka littoral cell may influence the patterns of shoreline change, and this complicates identifying sediment sources for any given shoreline stretch.

Extreme weather can change shorelines considerably over a short period of time. El Niño and La Niña events often increase the intensity of winter storms, which can cause visible erosion. Although data from the North Coast has not been analyzed, El Niño has been associated with wave direction shifts, high wave energy flux, elevated water levels, and coastal erosion on the North American west coast from California to British Columbia (Barnard et al. 2015). Intense El Niño and La Niña events (Appendix B: Table 2) might have influenced the widespread erosion in the study intervals 1971-1981 and 1988-1999. More detailed documentation of ENSO-related storm erosion or other events would be needed to conclusively tie climate events to shoreline changes seen in these intervals, however.

Conclusion

With the exception of the eroding shoreline at the North Jetty, the long-term trend in shoreline movement in the Humboldt Bay area shows the foredune foot maintaining the equilibrium with sea level, or building out toward the ocean. However, high rates of local relative sea level rise and global predictions of increasing rates of sea level rise over the 21st Century underscore the importance of continued study of shoreline change in the Humboldt Bay area. The sandy shorelines of the Eureka littoral cell offer important habitat, ecosystem services, recreation value, and protect low-lying infrastructure. Mechanisms of shoreline change in the Humboldt Bay area that merit additional study include littoral drift patterns, sources of vertical land motion, shoreline responses to climate events, the role of vegetation in dune translation, and sediment management. In association with an analysis of shorelines in the Eel River area, the Humboldt Bay Historical Shoreline Analysis can provide context for ongoing studies of dune evolution and coastal processes in the Eureka littoral cell.

References

Barnard, P.L., Revell, D.L., Hoover, D., Warrick, J., Brocatus, J., Draut, A.E., Dartnell, P., Elias, E., Mustain, N., Hart, P.E. and Ryan, H.F., 2009. Coastal processes study of Santa Barbara and Ventura counties, California (No. 2009-1029). US Geological Survey.

Battiau-Queney, Y., Billet, J.F., Chaverot, S. and Lanoy-Ratel, P., 2003. Recent shoreline mobility and geomorphologic evolution of macrotidal sandy beaches in the north of France. Marine geology, 194(1), pp.31-45.

Boak, E.H. and Turner, I.L., 2005. Shoreline Definition and Detection: A Review. Journal of Coastal Research: Volume 21, Issue 4: pp. 688 – 703.

Chaaban, F., Darwishe, H., Battiau-Queney, Y., Louche, B., Masson, E., El Khattabi, J. and Carlier, E., 2012. Using ArcGIS® modelbuilder and aerial photographs to measure coastline retreat and advance: North of France. Journal of Coastal Research, 28(6), pp.1567-1579.

Cayan, D.R., Bromirski, P.D., Hayhoe, K., Tyree, M., Dettinger, M.D. and Flick, R.E., 2008. Climate change projections of sea level extremes along the California coast. Climatic Change, 87, pp.57-73.

Davidson-Arnott, R.G., 2005. Conceptual model of the effects of sea level rise on sandy coasts. Journal of Coastal Research, pp.1166-1172.

Del Río, L. and Gracia, F.J., 2013. Error determination in the photogrammetric assessment of shoreline changes. Natural hazards, 65(3), pp.2385-2397.

Fletcher, C.H., Romine, B.M., Genz, A.S., Barbee, M.M., Dyer, Matthew, Anderson, T.R., Lim, S.C., Vitousek, Sean, Bochicchio, Christopher, and Richmond, B.M., 2012, National assessment of shoreline change: Historical shoreline change in the Hawaiian Islands: U.S. Geological Survey Open-File Report 2011–1051, 55 p. (Also available at https://pubs.usgs.gov/of/2011/1051.)

Gibbs, A.E. and Richmond, B.M., 2015. National assessment of shoreline change—Historical shoreline change along the north coast of Alaska, US–Canadian border to Icy Cape. US Geological Survey Open-File Report, 1048, p.96.

Hapke, C.J., Himmelstoss, E.A., Kratzmann, M.G., List, J.H., and Thieler, E.R., 2011, National assessment of shoreline change; historical shoreline change along the New England and Mid-Atlantic coasts: U.S. Geological Survey Open-File Report 2010-1118, 57 p., available at https://pubs.usgs.gov/of/2010/1118/.

Hapke, C.J., Reid, D., Richmond, B.M., Ruggiero, P., and List, J., 2006, National assessment of shoreline change: Part 3: Historical shoreline changes and associated coastal land loss along the sandy shorelines of the California coast: U.S. Geological Survey Open-file Report 2006-1219.

Hapke, C.J., Reid, D., 2007. National Assessment of Shoreline Change: Part 4, Historical Coastal Cliff Retreat along the California Coast: U.S. Geological Survey Open-File Report 2007-1133.

Hesp, P.A., 1983. Morphodynamics of incipient foredunes in NSW, Australia. In: Brookfield, M.E., Ahlbrandt, T.S. (Eds.), Eolian Sediments and Processes. Elsevier, Amsterdam, pp.325–342.

Hesp, P.A., 1984. The formation of sand ‘‘beach ridges’’ and foredunes. Search 15, 289–291.

Hesp, P.A. 2002. Foredunes and Blowouts: Initiation, Geomorphology and Dynamics. Geomorphology 48 (1–3): 245–68.

Hesp, P.A. 2013. A 34 year record of foredune evolution, Dark Point, NSW, Australia. Journal of Coastal Research (65): 1-7.

Himmelstoss, E.A. 2009. “DSAS 4.0 Installation Instructions and User Guide” in: Thieler, E.R., Himmelstoss, E.A., Zichichi, J.L., and Ergul, Ayhan. 2009 Digital Shoreline Analysis System (DSAS) version 4.0 — An ArcGIS extension for calculating shoreline change: U.S. Geological Survey Open-File Report 2008-1278. *updated for version 4.3.

IPCC. 2014. Climate Change 2014: Synthesis Report. Contribution of Working Groups I, II and III to the Fifth Assessment Report of the Intergovernmental Panel on Climate Change [Core Writing Team, R.K. Pachauri and L.A. Meyer (eds.)]. IPCC, Geneva, Switzerland, 151 pp.

Laird, A. 2007. Historical Atlas of Humboldt Bay and Eel River Delta. Prepared for Humboldt Bay Harbor, Recreation and Conservation District, Eureka CA. Trinity Associates, Arcata, CA.

McDonald, K. 2014. Differences in the morphology of restored and invaded foredunes, Humboldt Bay, California. Unpubished report, Humboldt Bay National Wildlife Refuge, Arcata, California.

Moffat & Nichol. 2013. Coastal Regional Sediment Management Plan, Eureka Littoral Cell, California. Prepared for California Coastal Sediment Management Workgroup. USACE.

Moore, L.J. 2000. Shoreline Mapping Techniques. Journal of Coastal Research, 16(1). 111-124.

Morton, Robert A., Miller, Tara L., and Moore, Laura J., 2004, National assessment of shoreline change: Part 1: Historical shoreline changes and associated coastal land loss along the U.S. Gulf of Mexico: U.S. Geological Survey Open-file Report 2004-1043, 45p

Morton, R. A., and Miller, T. L., 2005, National assessment of shoreline change: Part 2: Historical shoreline changes and associated coastal land loss along the U.S. Southeast Atlantic Coast: U.S. Geological Survey Open-file Report 2005-1401.

National Research Council (NRC). 2012. Sea-Level Rise for the Coasts of California, Oregon, and Washington: Past, Present, and Future. Washington, DC: The National Academies Press. https://doi.org/10.17226/13389.

NOAA Center for Weather and Climate Prediction, Climate Prediction Center Internet Team. “Cold and Warm Episodes by Season”. Accessed July 2017. http://www.cpc.ncep.noaa.gov/products/analysis_monitoring/ensostuff/ensoyears.shtml

Northern Hydrology & Engineering. 2015. Humboldt Bay: Sea Level Rise, Hydrodynamic Modeling, and Inundation Vulnerability Mapping, Prepared for State Coastal Conservancy, and Coastal Ecosystems Institute of Northern California. McKinleyville, CA.

Pajak, M.J., and Leatherman, S., 2002. The high water line as shoreline indicator. Journal of Coastal Research, 18(2),329-337.

Patsch, K. and G. Griggs. 2007. Development of Sand Budgets for California’s Major Littoral Cells. Institute of Marine Sciences, University of California, Santa Cruz, California Department of Boating and Waterways, California Coastal Sediment Management Workgroup.

Patton, J. R., T. B. Williams, J. K. Anderson, R. Burgette, and T. Leroy. 2017. Tectonic land level changes and their contribution to sea-level rise, Humboldt Bay region, Northern California: 2017 Final Report. Prepared for U.S. Fish and Wildlife Service Coastal Program. CascadiaGeoSciences, McKinleyville, CA.

Pickart, A.J. and Sawyer, J.O., 1998. Ecology and restoration of northern California coastal dunes. California Native Plant Society.

Pickart, A.J. 2014. Dune Restoration and Shoreline Change, Humboldt Bay, California. USFWS.

Thieler, E.R. and Danforth, W.W. 1994. Historical Shoreline Mapping (I): Improving Techniques and Reducing Positioning Errors. Journal of Coastal Research, 10(3) p549-563.

Thieler, E.R., Himmelstoss, E.A., Zichichi, J.L., and Ergul, Ayhan, 2017, Digital Shoreline Analysis System (DSAS) version 4.0—An ArcGIS extension for calculating shoreline change (ver. 4.4, July 2017): U.S. Geological Survey Open-File Report 2008-1278, https://pubs.er.usgs.gov/publication/ofr20081278

Trenberth, Kevin & National Center for Atmospheric Research Staff (Eds). Last modified 02 Feb 2016. "The Climate Data Guide: Nino SST Indices (Nino 1+2, 3, 3.4, 4; ONI and TNI)." Retrieved from https://climatedataguide.ucar.edu/climate-data/nino-sst-indices-nino-12-3-34-4-oni-and-tni.

U.S. Army Corps of Engineers (USACE). 2012. Five- Year Programmatic Environmental Assessment and 404 (b)(1) Analysis, Humboldt Harbor and Bay Operations and Maintenance, Dredging (FY 2012- FY 2016), Humboldt Bay, Humboldt County, California.

U.S. Army Corps of Engineers (USACE). 2017. Humboldt Harbor and Bay Federal Navigation Channels Calendar Years 2017-2020 Maintenance Dredging Consistency Determination (CD-0002-17).

Appendix A. Maps by Shoreline Stretch

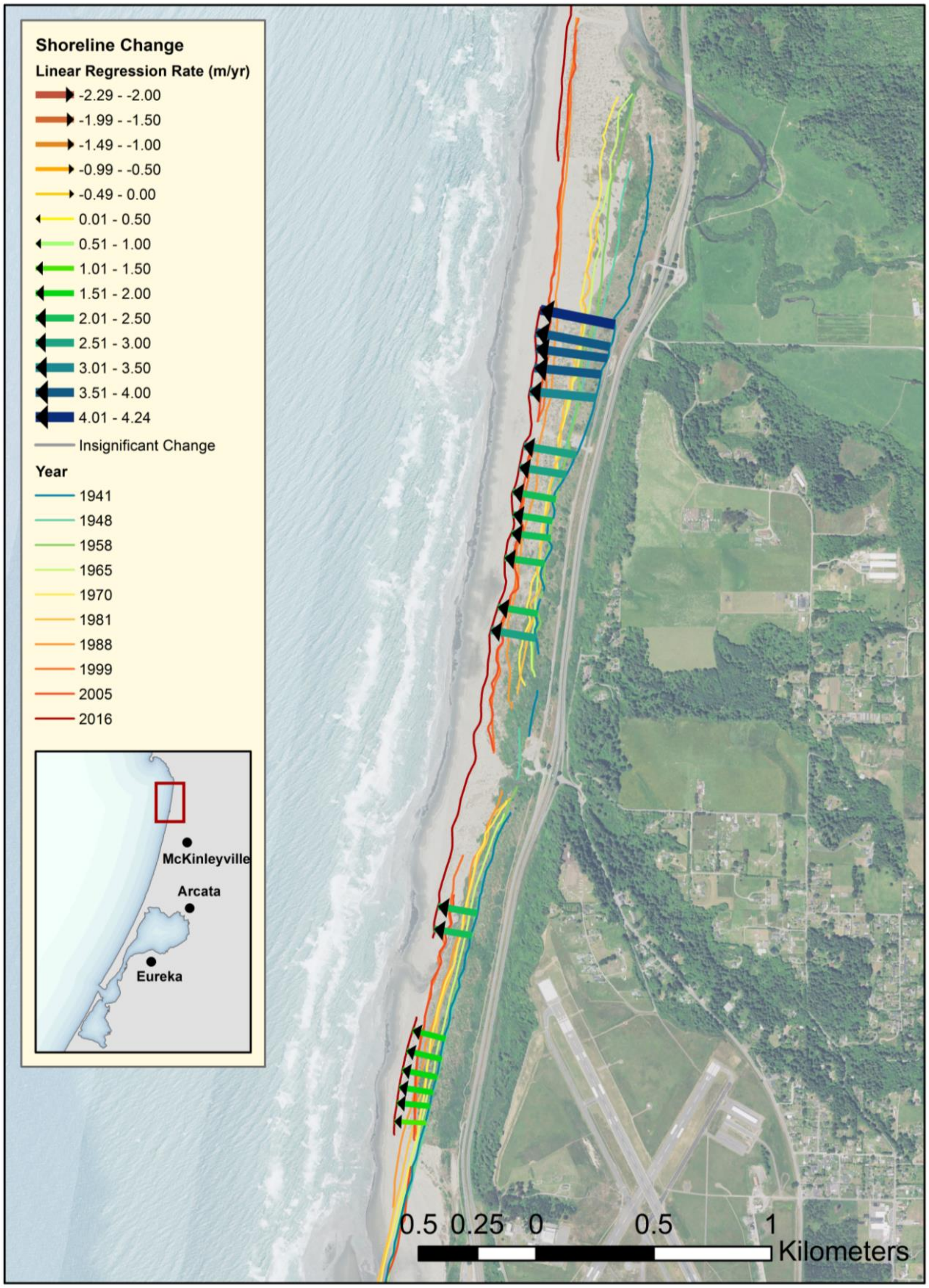

Figure 1. The Clam Beach to Little River study area showed high rates of accretion from 1941-2016, with linear regression rates of change along transects ranging from 1.42 m/year to 4.24 m/year.

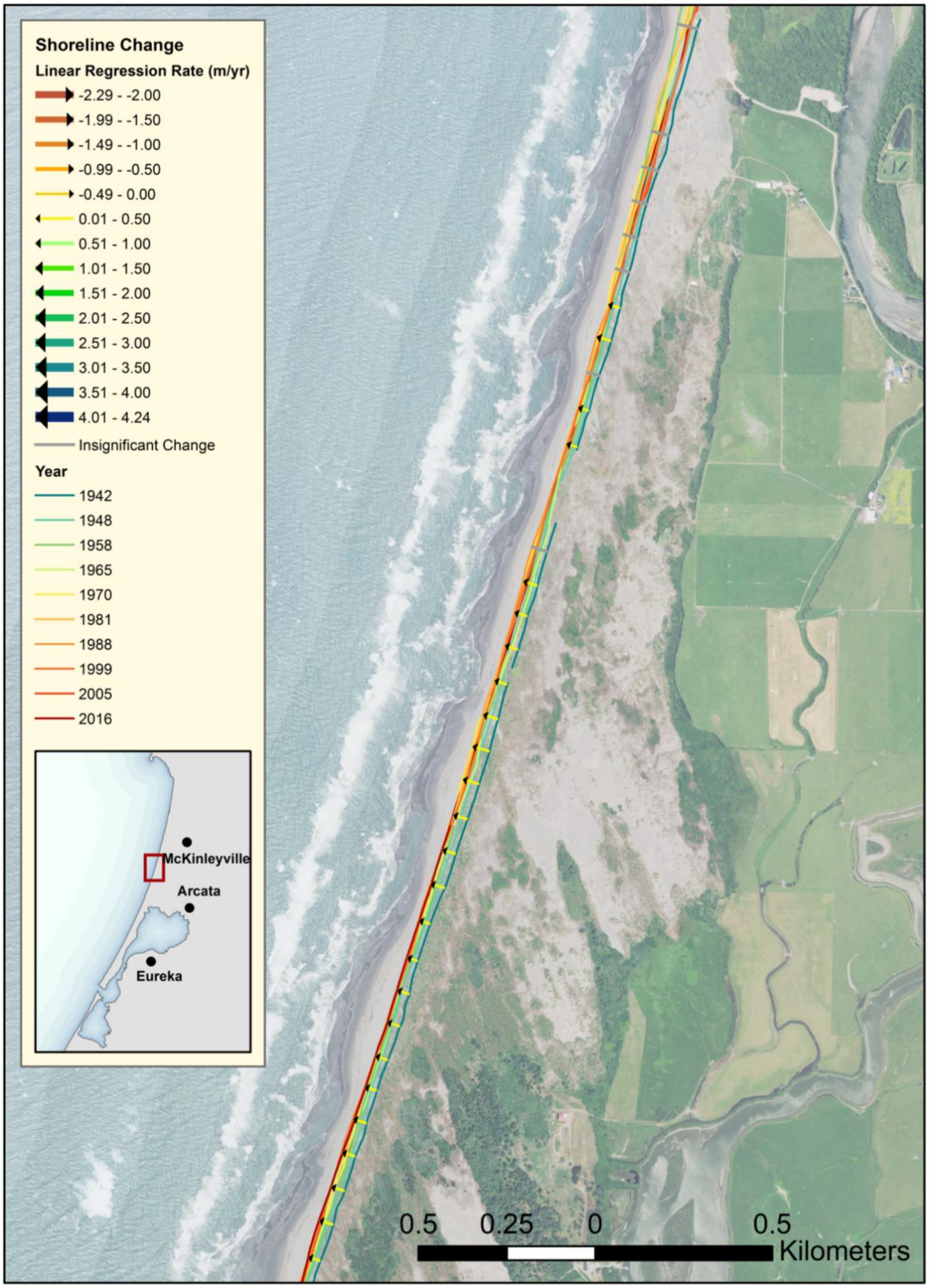

Figure 2. The Mad River Beach study area showed no change to low accretion from 1941-2016, with linear regression rates of change along transects ranging from 0.04 m/year (no significant change) to 0.46 m/year.

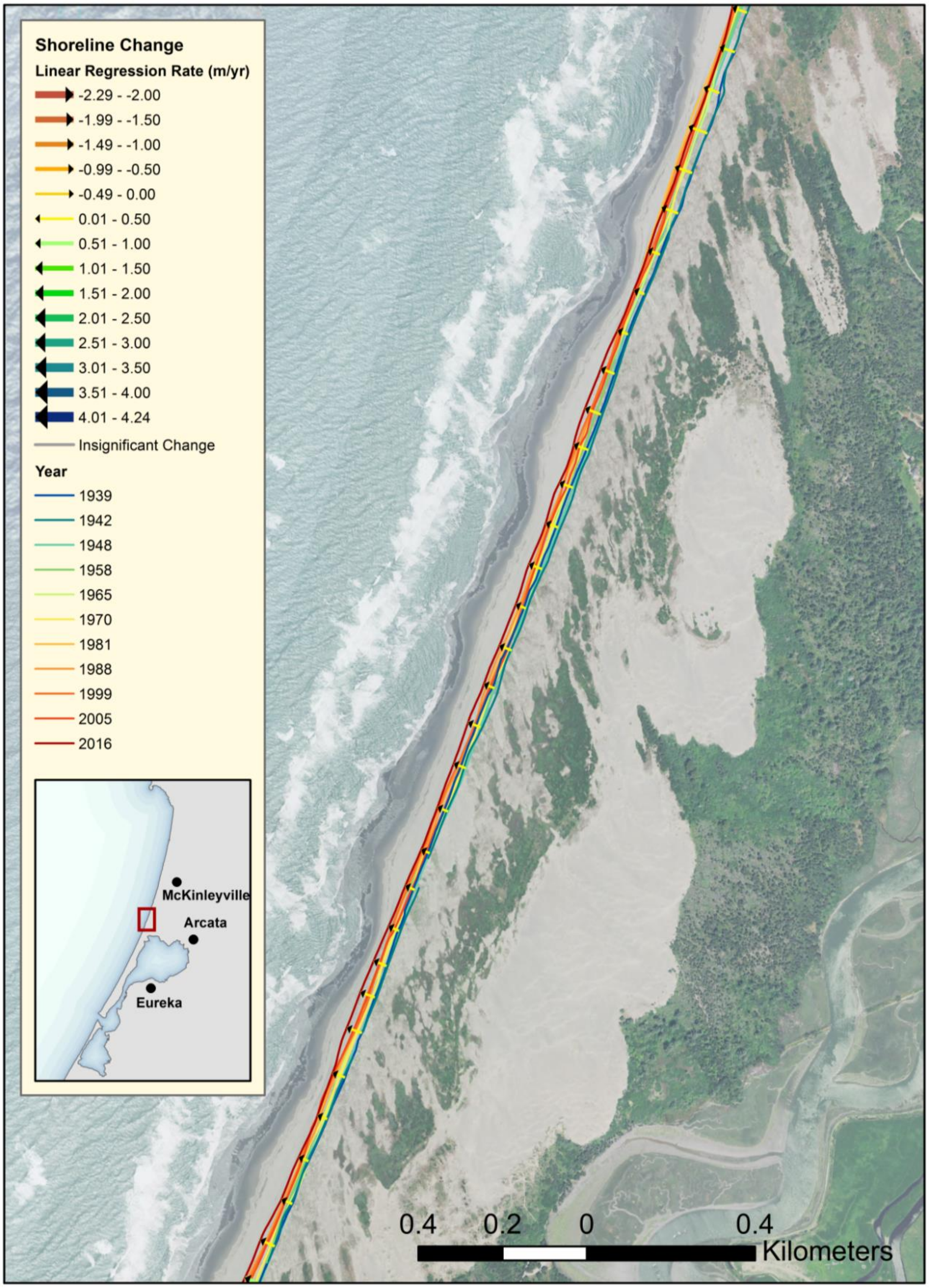

Figure 3. The Lanphere-Ma-le'l study area showed small but significant rates of accretion from 1939-2016, with linear regression rates of change along transects ranging from 0.21 m/year to 0.44 m/year.

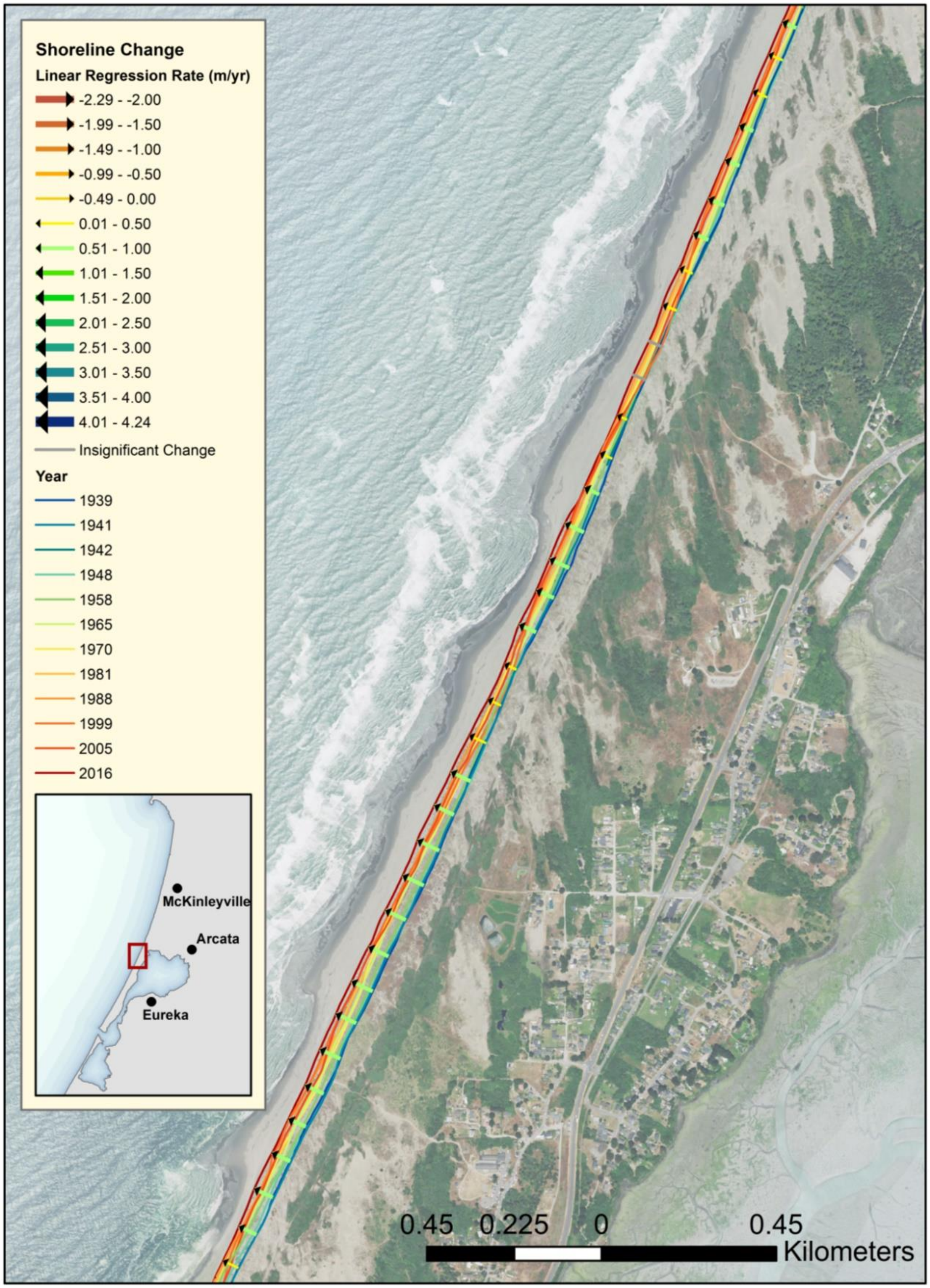

Figure 4. The Manila study area showed no change to low accretion from 1939-2016, with linear regression rates of change along transects ranging from 0.24 m/year (no significant change) to 0.76 m/year.

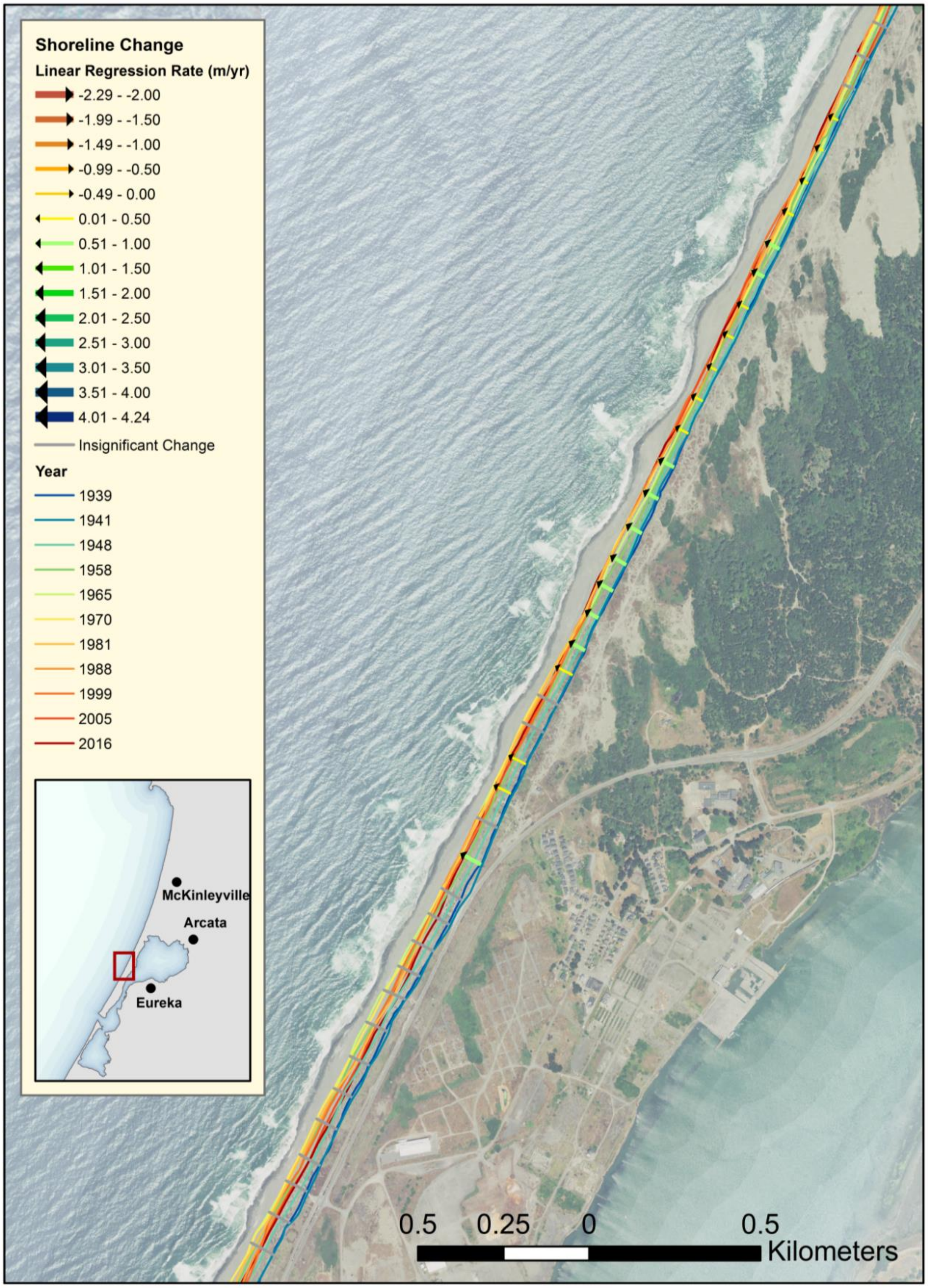

Figure 5. The Samoa study area showed no change to low accretion from 1939-2016, with linear regression rates of change along transects ranging from 0.07 m/year (no significant change) to 0.69 m/year.

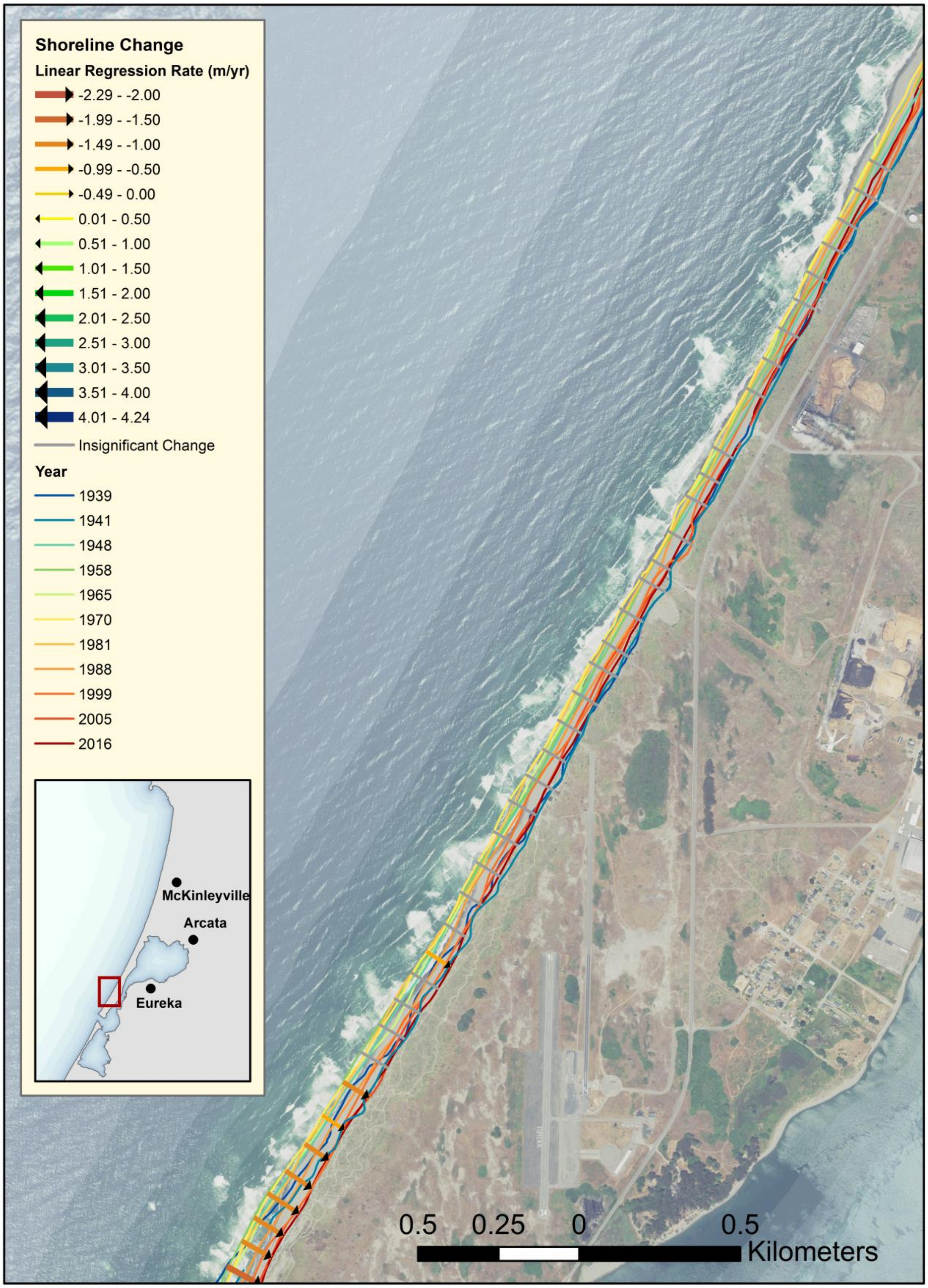

Figure 6. The Fairhaven study area showed no change to medium erosion from 1939-2016, with linear regression rates of change along transects ranging from -0.04 m/year (no significant change) to -1.42 m/year. The Fairhaven shoreline shows high fluctuation, with an average shoreline change envelope of 80.59 m.

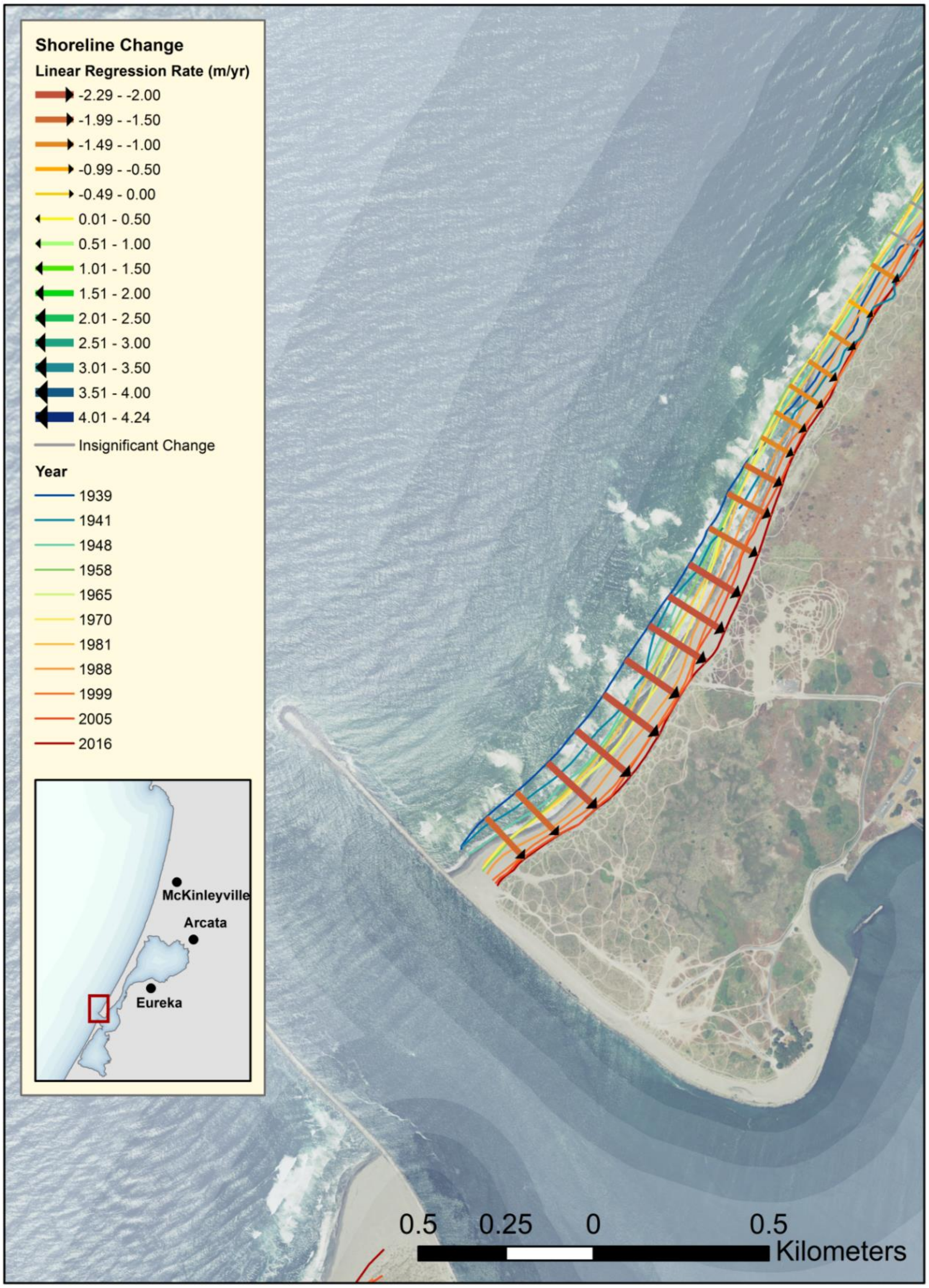

Figure 7. The North Jetty study area showed high erosion from 1939-2016, with linear regression rates of change along transects ranging from -1.68 m/year to -2.29 m/year and as much as 200 m of erosion.

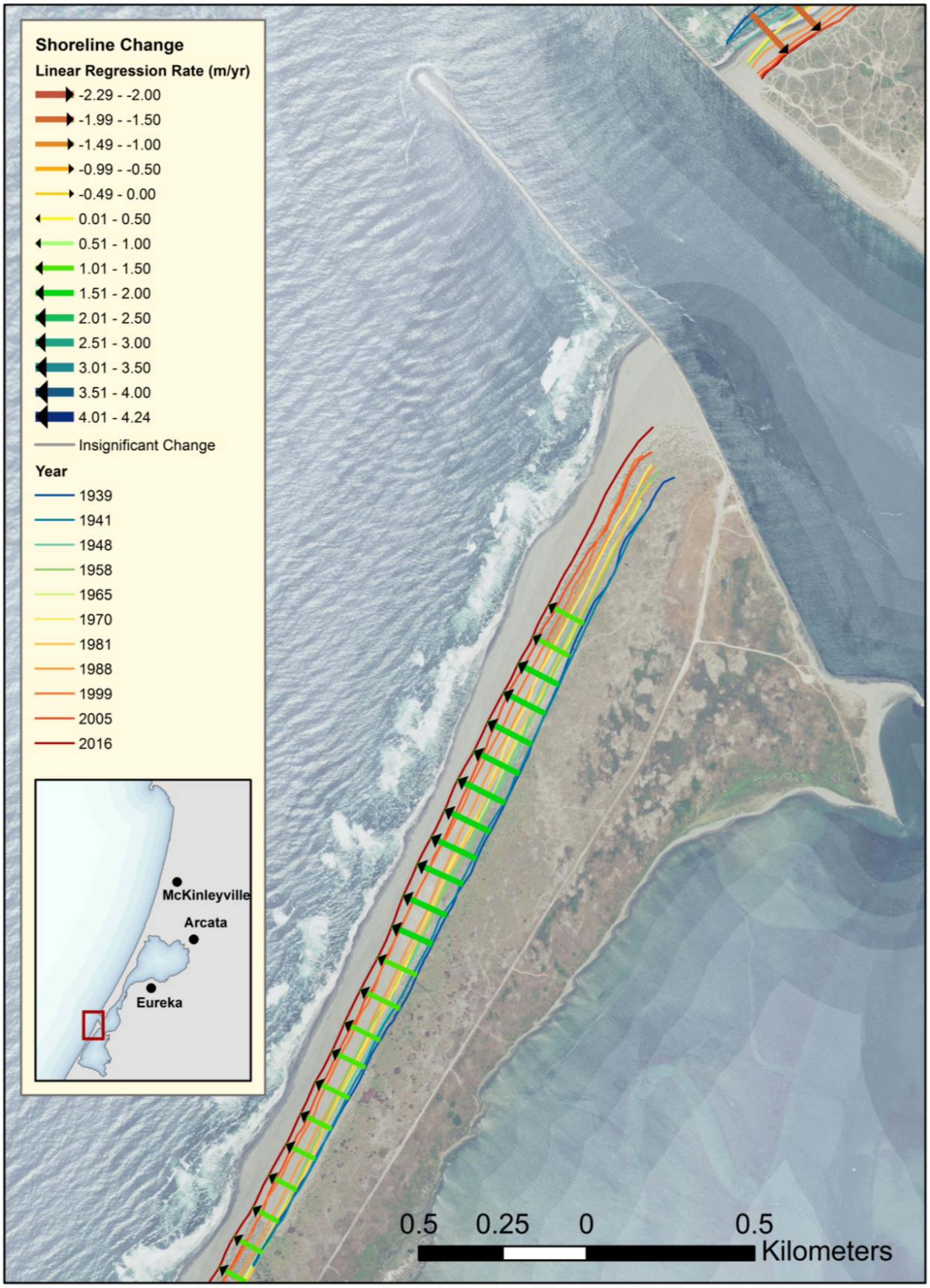

Figure 8. The South Jetty study area showed medium accretion from 1939-2016, with linear regression rates of change along transects ranging from 1.13 m/year to 1.82 m/year and as much as 157 m of accretion.

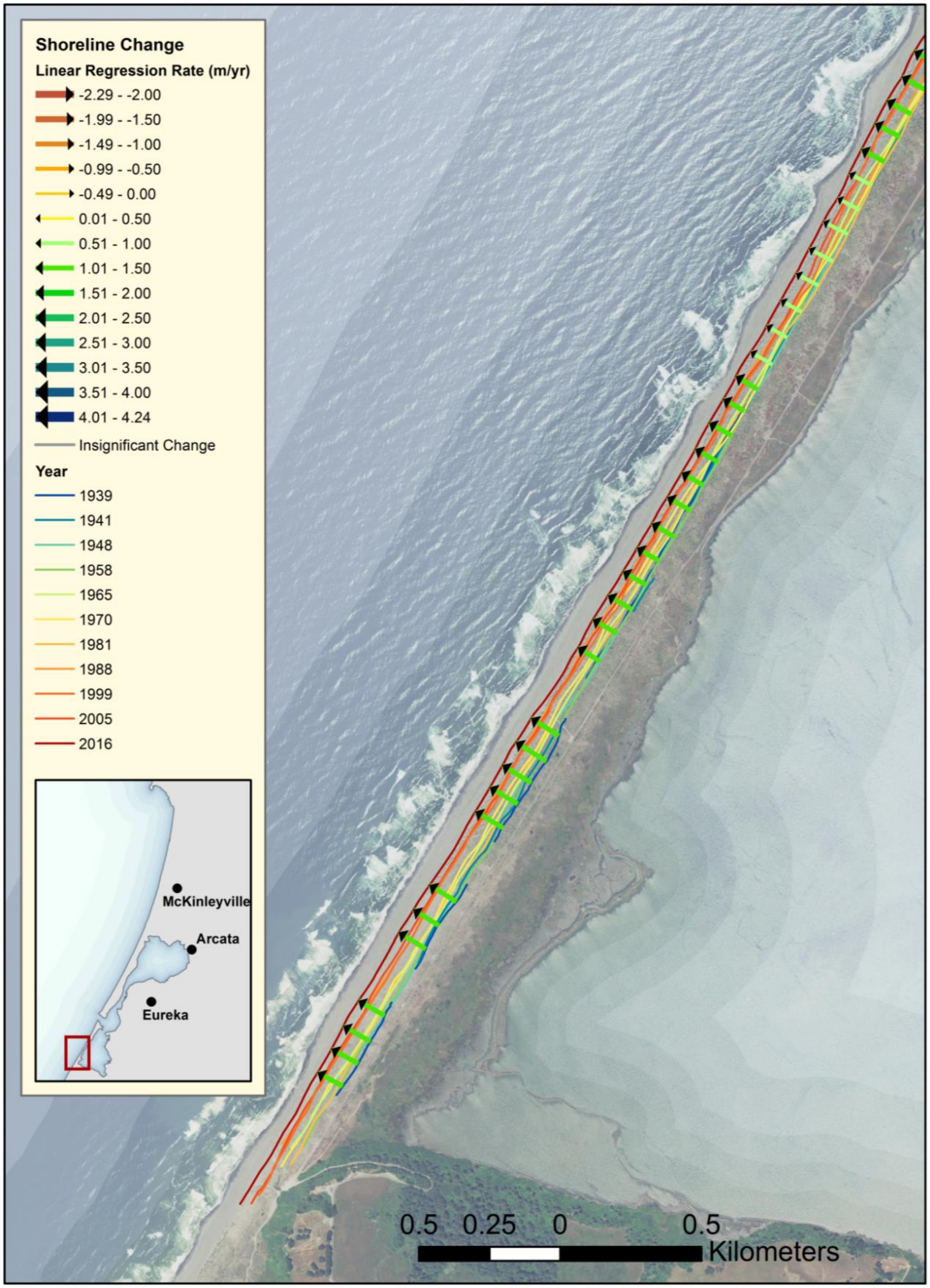

Figure 9. The South Spit to Table Bluff study area showed low to medium accretion from 1939-2016, with linear regression rates of change along transects ranging from 0.71 m/year to 1.47 m/year and as much as 127 m of accretion.

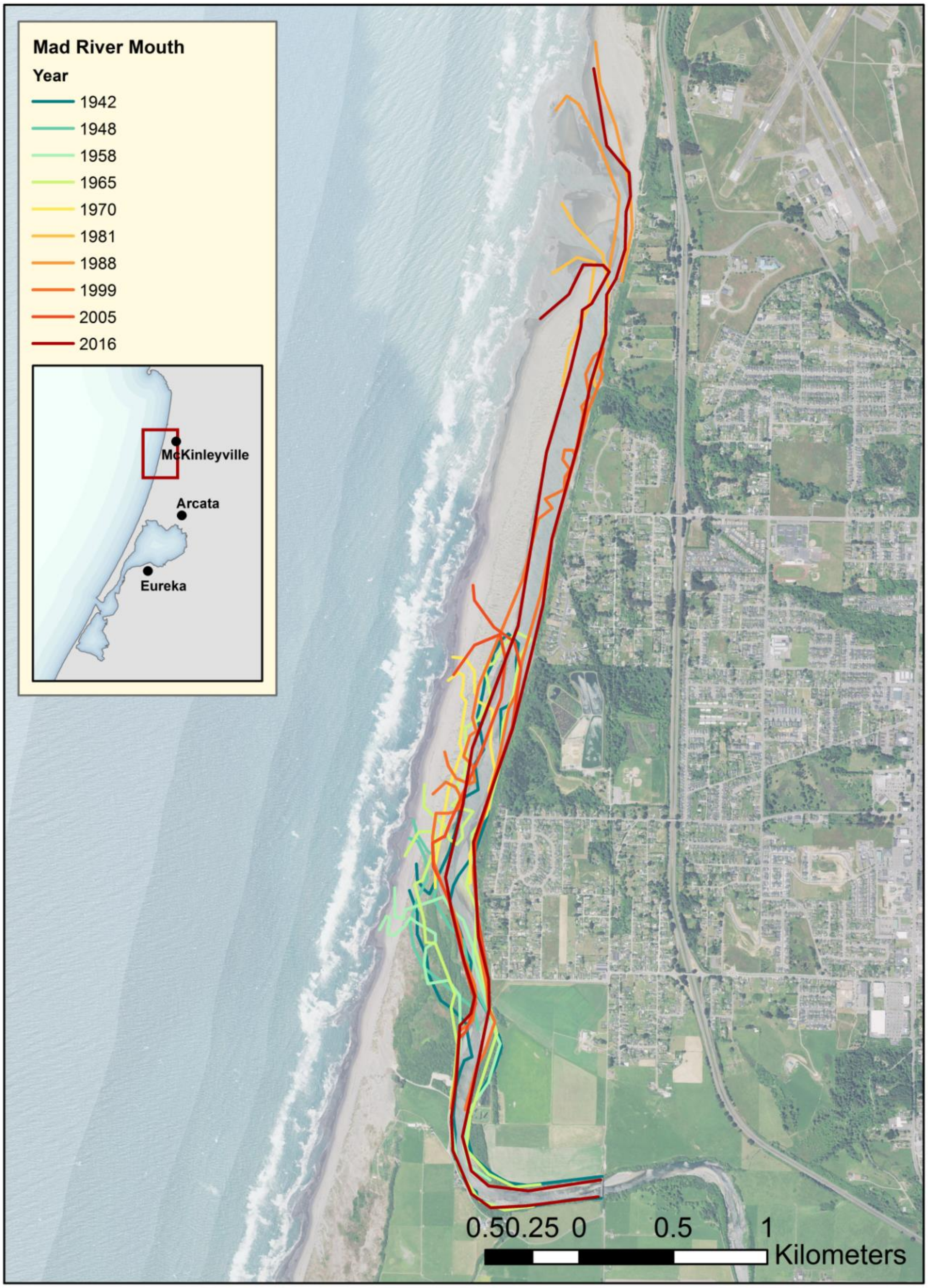

Figure 10. The Mad River Mouth has fluctuated over 4.75 km over the study period. The Mad River Mouth area was not included in the shoreline analysis because the shorelines are discontinuous.

Appendix B. Source Data and Meteorological Data

Year	Imagery Source	Data Type	Start_Date	End_Date	Season	Rectification	Resolution	Extent	Color	Scale
1939	Humboldt County Public Works	Scanned Aerial Photos	12/21/1939	12/21/1939	Winter	Georeferenced	600dpi scan	Table Bluff to Lanphere	BW	~1:10,000
1941/42	Humboldt County Public Works	Scanned Aerial Photos	11/23/1941	2/16/1942	Winter	Georeferenced	600dpi scans	South Spit to Little River	BW	1:20,000
1948	Humboldt Bay Historical Atlas	Aerial Photo Mosaic	6/22/1948	6/22/1948	Summer	Orthorectified	600 dpi scan	Table Bluff to Mad River	BW	~1:20,000
1948	Humboldt County Public Works	Scanned Aerial Photos	6/23/1948	6/23/1948	Summer	Georeferenced	600dpi scan	Mad River to Little River	BW	~1:20,000
1958	Humboldt Bay Historical Atlas	Aerial Photo Mosaic	8/12/1958	8/12/1958	Summer	Orthorectified	600 dpi scan	Table Bluff to Mad River	BW	1:12,000
1958	Humboldt County Public Works	Scanned Aerial Photos	8/1/1958	9/2/1958	Summer	Georeferenced	1200 ppi	Mad River to Little River	BW	1:12,000
1965	Humboldt Bay Historical Atlas	Aerial Photo Mosaic	7/27/1965	8/29/1965	Summer	Orthorectified	600 dpi scan	Table Bluff to Mad River	BW	1:20,000
1965	Humboldt County Public Works	Scanned Aerial Photos	8/29/1965	8/29/1965	Summer	Georeferenced	800 dpi	Mad River to Little River	BW	1:20,000
1970	Humboldt Bay Historical Atlas	Aerial Photo Mosaic	9/9/1970	9/9/1970	Early Fall	Orthorectified	600 dpi scan	Table Bluff to Mad River	BW	~1:12,000
1970	Humboldt County Public Works	Scanned Aerial Photos	7/21/1970	7/21/1970	Summer	Georeferenced	600dpi scan	Mad River to Little River	BW	~1:12,000
1981	Humboldt Bay Historical Atlas	Aerial Photo Mosaic	6/15/1981	6/15/1981	Summer	Orthorectified	600 dpi scan	Table Bluff to Mad River	BW	1:24,000
1981	Humboldt County Public Works	Scanned Aerial Photos	6/15/1981	6/15/1981	Summer	Georeferenced	600 dpi scan	Mad River to Little River	BW	1:24,000
1988	National Digital Ortho Photo Program	Digital Orthoimagery Mosaic	3/30/1988	3/30/1988	Spring	Orthorectified by APFO	1m	Extent of Study Area	BW	1:40,000
1999	Humboldt County Public Works	Scanned Aerial Photos	11/13/1999	11/13/1999	Winter	Georeferenced	600ppi	Extent of Study Area	Color	1:6,000
2005	National Agriculture Imagery Program	Digital Orthoimagery Mosaic	6/15/2005	6/29/2005	Summer	Orthorectified by APFO	1m	Extent of Study Area	Color	1:40,000
2016	National Agriculture Imagery Program	Digital Orthoimagery Mosaic	6/1/2016	6/30/2016	Summer	Orthorectified by APFO	1m	Extent of Study Area	Color	1:12,000

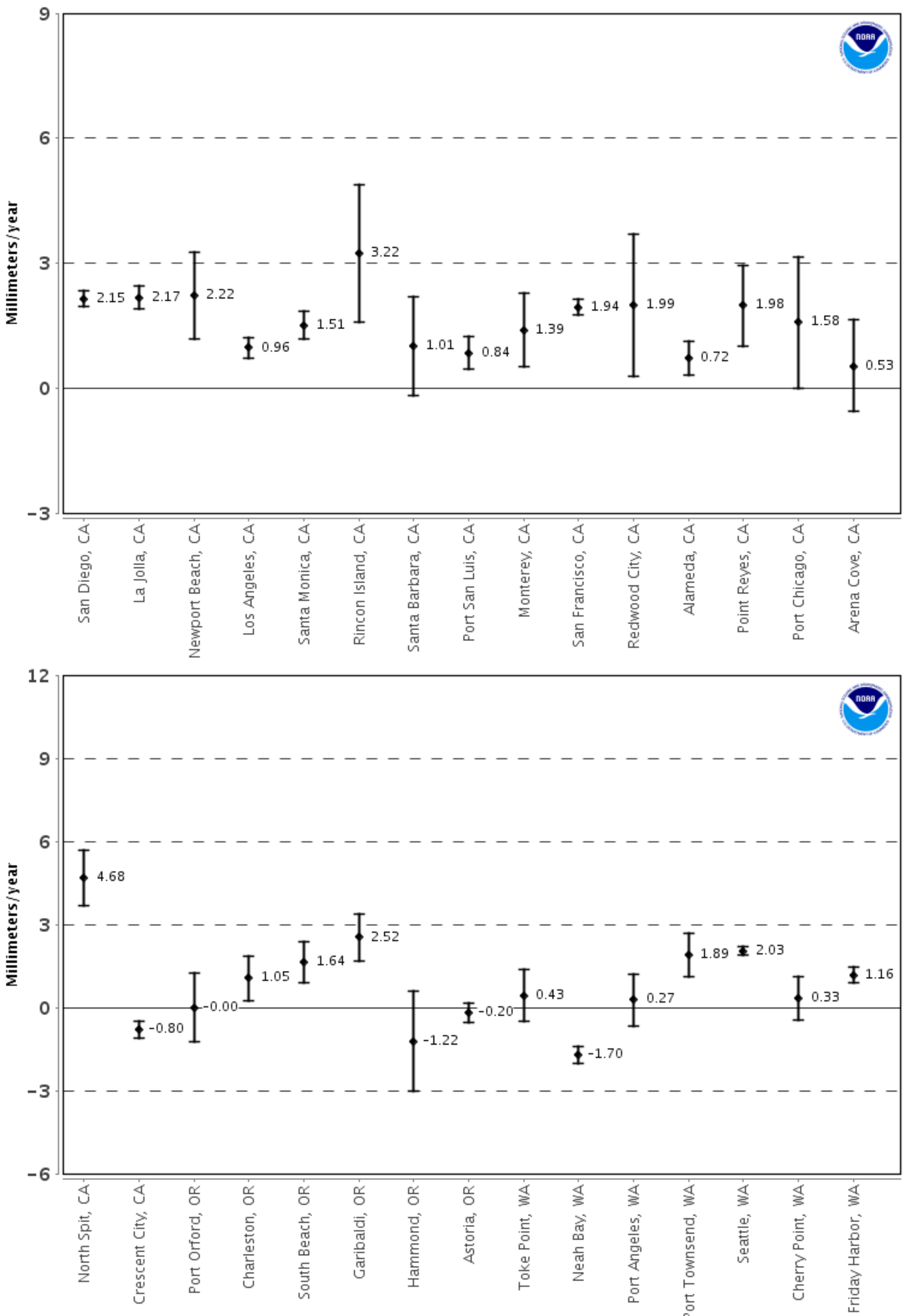

Figure 1. The North Spit tide gauge shows the highest rate of relative sea level rise on the Pacific Coast of the United States. Plots downloaded from NOAA CO-OPS on July 31, 2017.

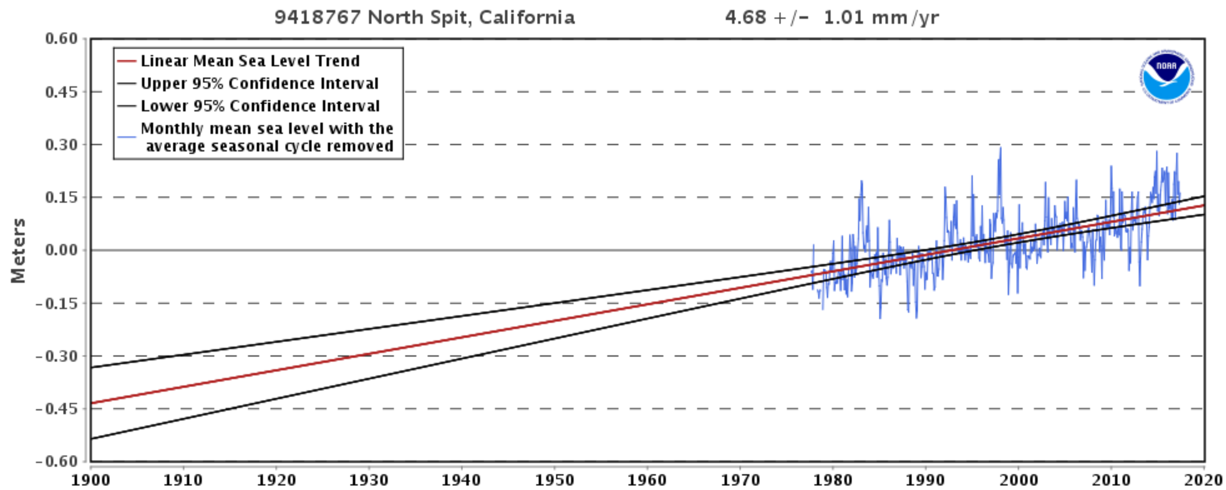

Figure 2. The North Spit tide gauge shows high relative sea level rise since 1977. Plots downloaded from NOAA CO-OPS on July 31, 2017.

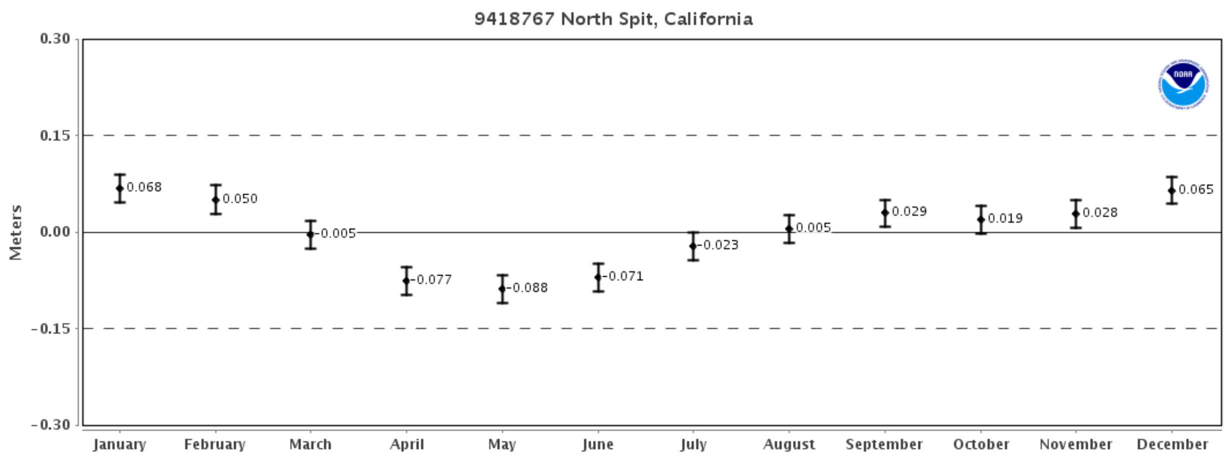

Figure 4. Sea level varies by season, with lower sea levels occurring during the spring upwelling that cools water temperature in the spring. Plot downloaded from NOAA CO-OPS July 31, 2017. Available at https://tidesandcurrents.noaa.gov/sltrends/northpacifictrends.htm.

Table 2. Documented climate events (1950-2017) period are provided with categorical intensities based on Oceanic Niño Index (ONI). El Niño and La Niña events are commonly defined using ONI as five consecutive months of 3-month mean sea surface temperature anomaly in the mid-Pacific equatorial region >0.5°C. The table shows *Strong* events with ONI >1.5°C and *Very Strong* events with ONI>2.0°C. The 1964 flood is included because the high levels of debris can be seen in 1965 aerial imagery, and the event could have impacted the shoreline, particularly around river mouths.

Climate Event	**Year**	**Intensity**
El Niño	1957-58	Strong
1964 Flood	1964-65	Other
El Niño	1965-66	Strong
El Niño	1972-73	Strong
La Niña	1973-74	Strong
La Niña	1975-76	Strong
El Niño	1982-83	Very Strong
La Niña	1988-89	Strong
El Niño	1997-98	Very Strong
El Niño	2015-16	Very Strong